Zona de Convergencia del Atlantico Sur

925 hPa Vector Wind, 200 hPa streamlines,
and Merged Gauge and Satellite Estimated Precipitation
December-February Mean (1979-1995)

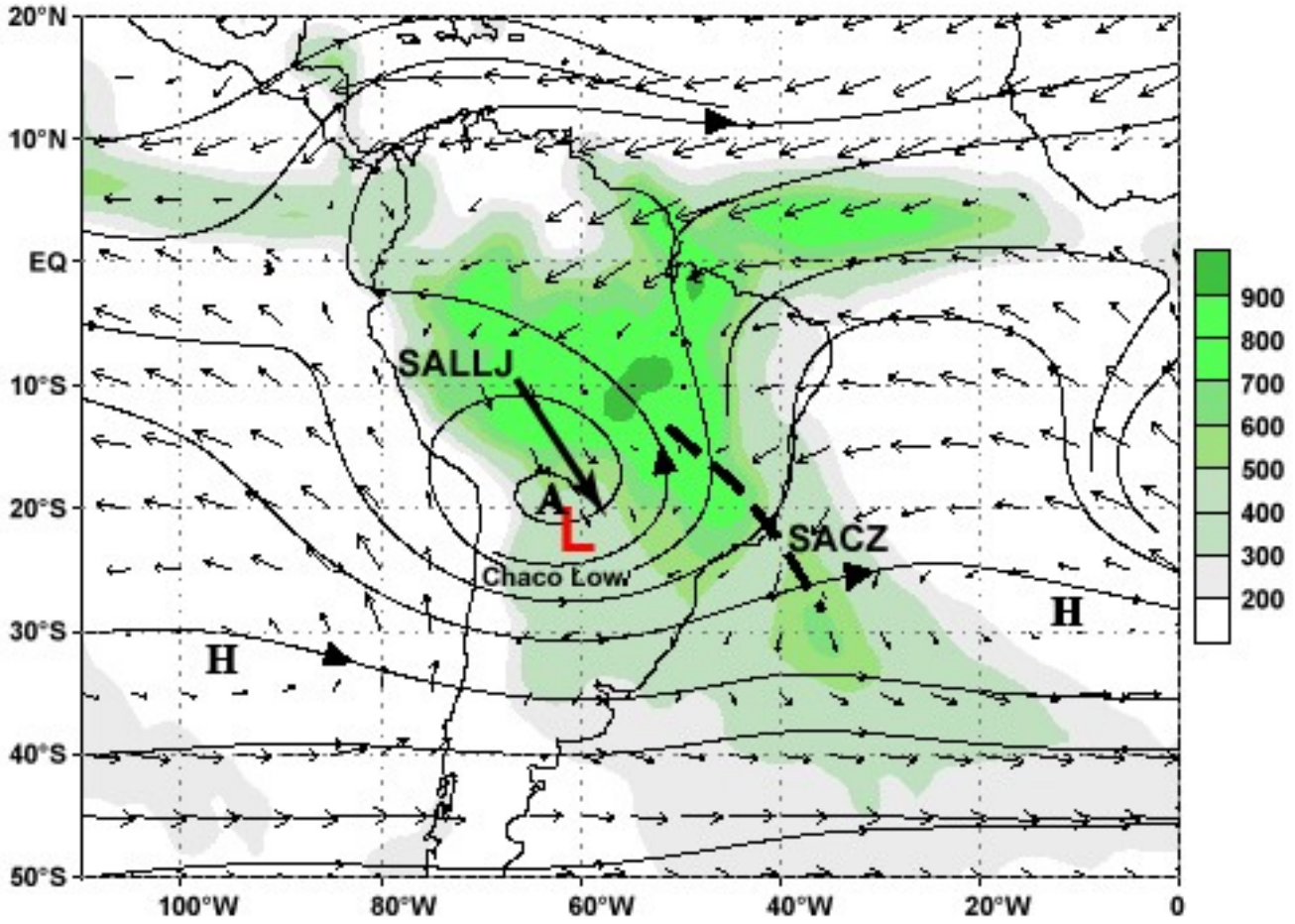

Courtesy of Vernon E. Kousky, NOAA/ Climate Prediction Center

- Kodama (1992) – Zonas de Precipitación Subtropical

Baiu-Meiyu Front

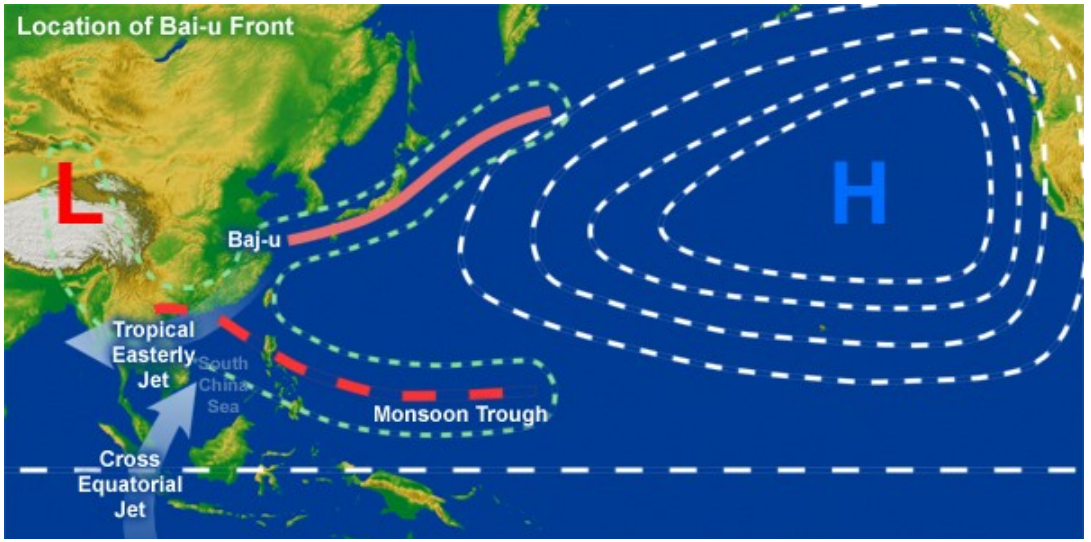

SACZ & SPCZ

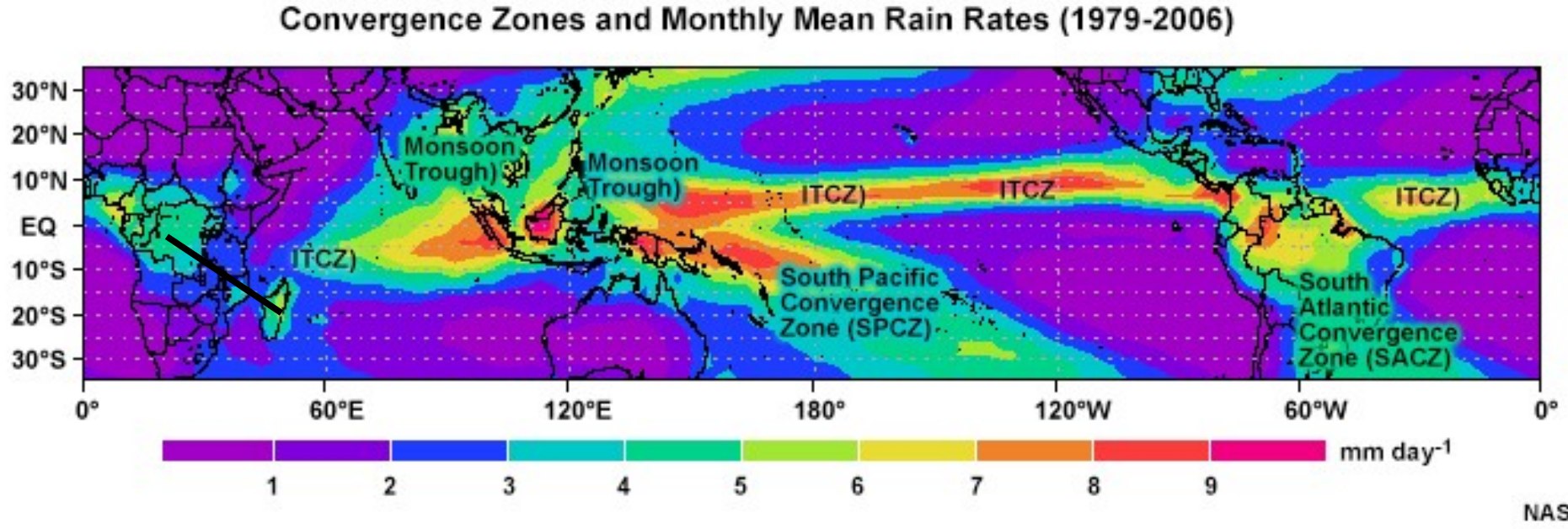

SICZ

Características de las ZPS:

- se forman a lo largo de las corrientes en chorro subtropicales al este de una vaguada cuasi-permanente situada al sureste de la zona de conveccion del monson asociado.

- son límites polares de la masa de aire húmedo de origen tropical.

- las lluvias intensas se mantienen por convergencia de humedad (5-10 mm/dia) transportada hacia la region por: una a lo largo de la ZPS y otra en dirección perpendicular asociada al anticiclon.

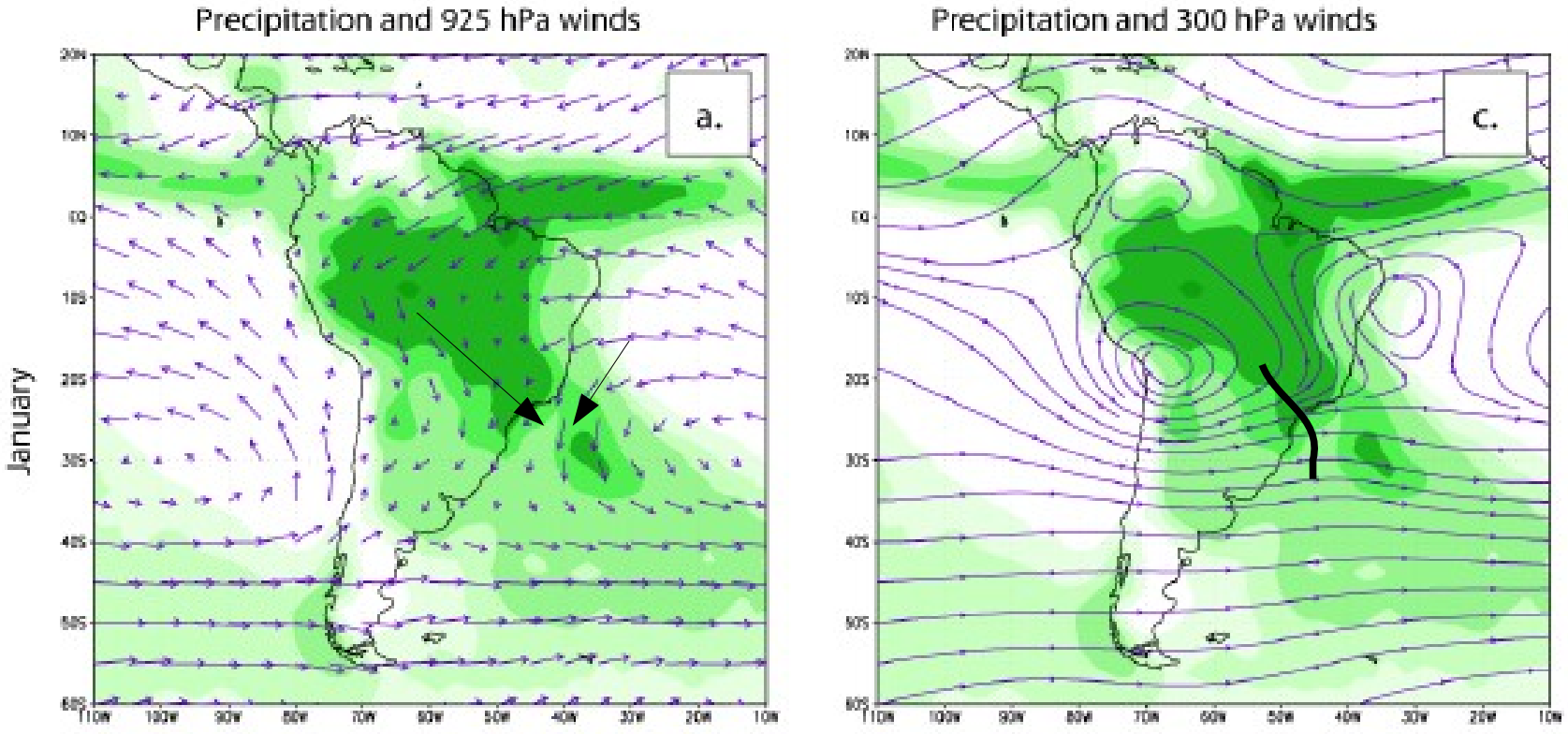

¿Por que la ZCAS se ubica en esa posición?

Continental heating effect

The Gill model for tropical convection: prescribed at equator

Solución estacionaria

$$\frac{\partial u}{\partial t} - \beta y v = -g\frac{\partial h'}{\partial x} - \frac{u}{\tau_D},$$

$$\frac{\partial v}{\partial t} + \beta y u = -g\frac{\partial h'}{\partial y} - \frac{v}{\tau_D},$$

$$\frac{\partial h'}{\partial t} = -h_0 \nabla \cdot \mathbf{v} + \mathcal{Q} - \frac{h'}{\tau_D}.$$

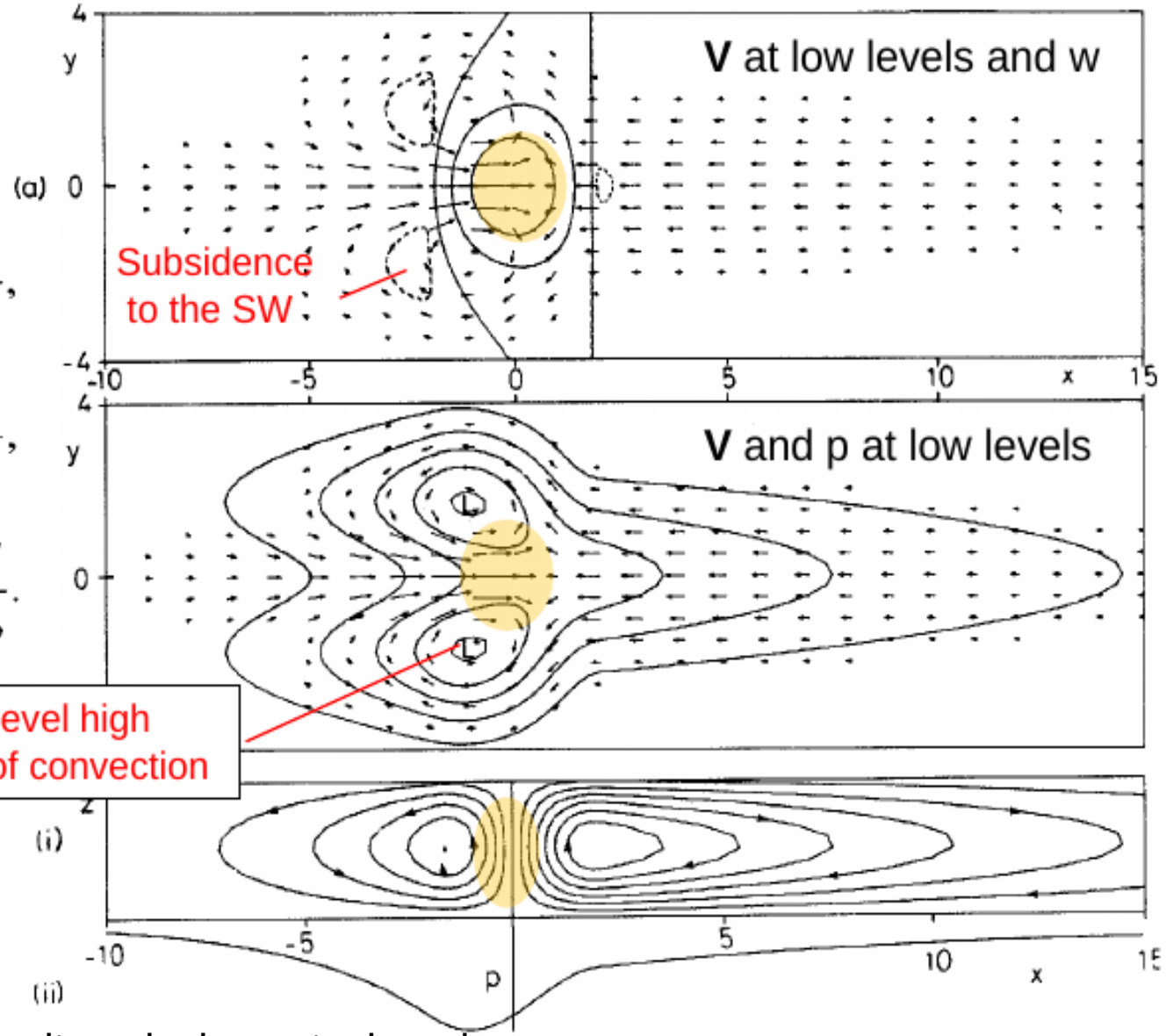

Tau_D= 5 dias permite solucion estacionaria

Gill 1980

Equatorial waves

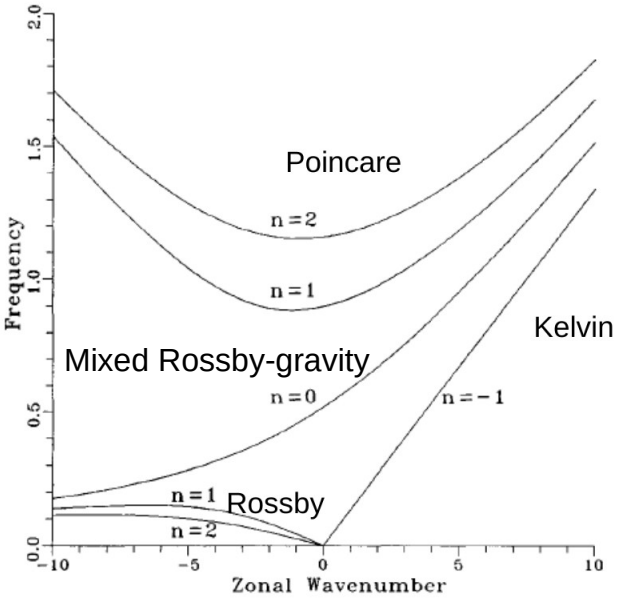

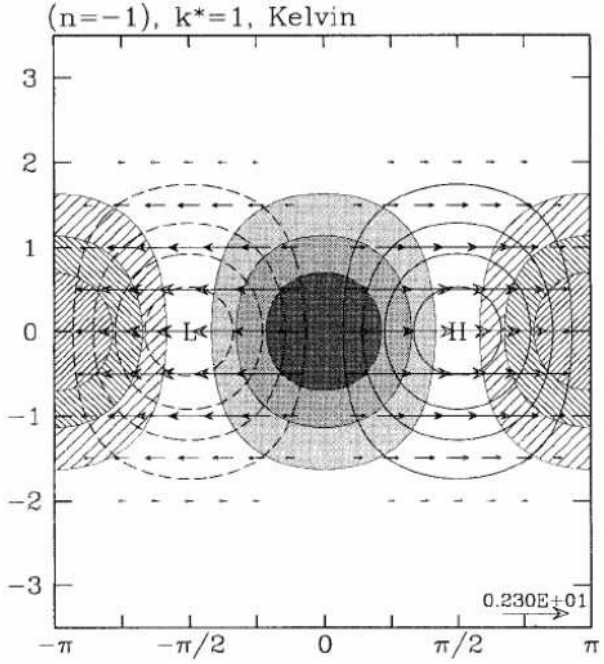

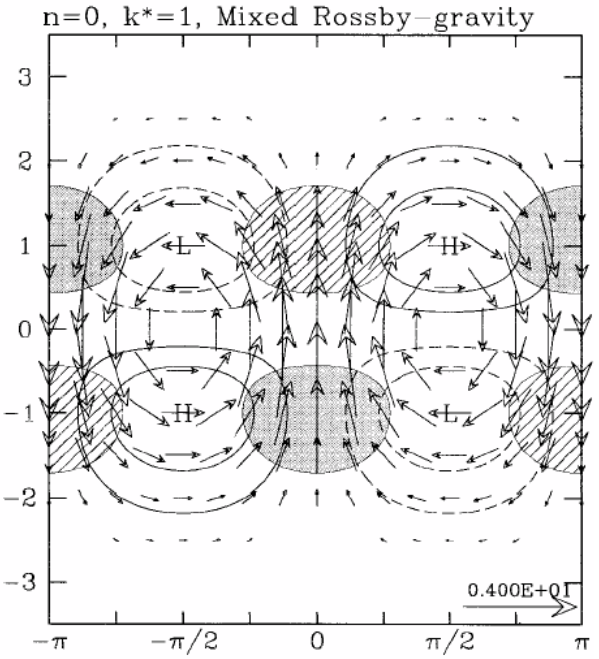

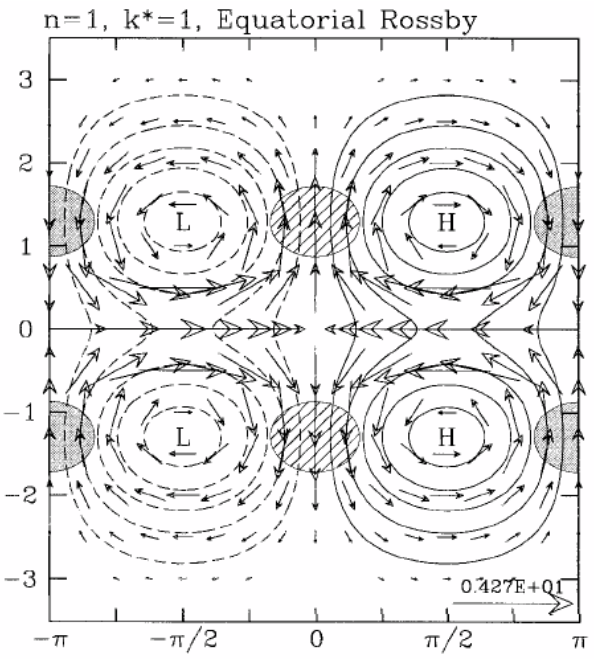

Si la fuente de calor se introduce al sur del Ecuador, la solucion de Gill es:

Solución en bajos niveles

b)

a)

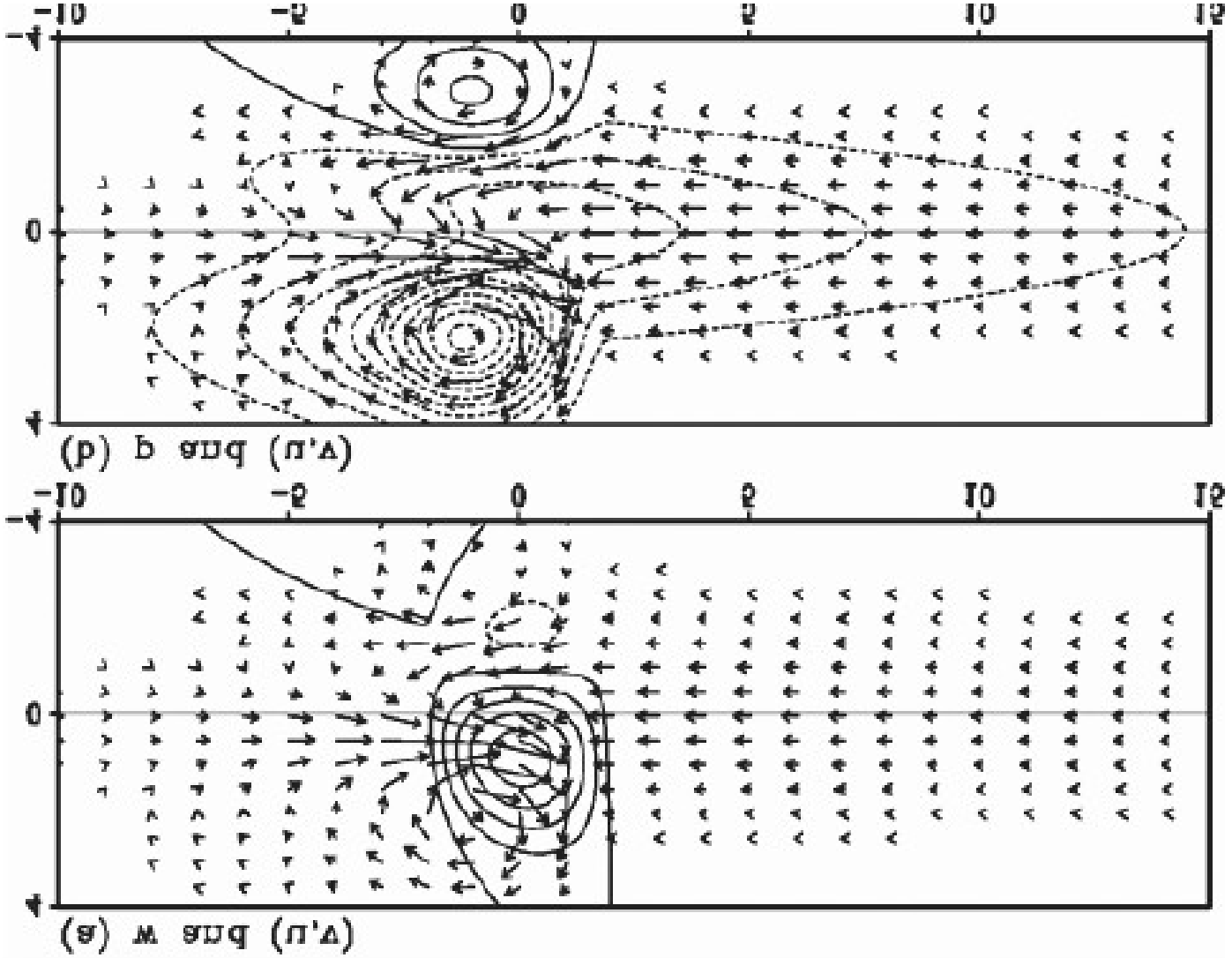

Gill's solution for atmospheric response to a "monsoon- like heating" in an idealized equatorial plane of longitude and latitude (units: 1000 km). (a) Upward motion (w, solid contours) is colocated with imposed heating at 0 longitude just south of the Equator. Low-level zonal (u) and meridional (v) winds respond to imposed heating, leading to convergence on the Equator and cyclonic circulations south of it, in a pattern that resembles the monsoons. (b) The response to the heating of surface pressure (p , contours, dashed for negative values) is in approximate geostrophic balance with near-surface winds.

Large-Scale Response of the Tropical Atmosphere to Transient Convection

PEDRO L. SILVA DIAS[1]

National Center for Atmospheric Research,[2] Boulder, CO 80307

WAYNE H. SCHUBERT AND MARK DEMARIA

Department of Atmospheric Science, Colorado State University, Fort Collins, CO 80523

(Manuscript received 7 February 1983, in final form 15 July 1983)

ABSTRACT

We consider the problem of the linear response of a stratified, equatorial, β-plane model atmosphere to specified transient sources of heat and momentum. The method of solution involves transforms in all three spatial coordinates. A finite Stürm-Liouville transform is used in z, a Fourier transform in x, and a generalized Hermite transform in y. The resulting spectral equations can then be solved analytically for a specified forcing. Of particular interest is the case of a Gaussian-shaped heat source centered at latitude y_o and with e-folding radius a. The heat source is transient and has time scale $1/\alpha$. Using the Parceval relation we compute how the forced energy is partitioned between Kelvin, mixed Rossby–gravity, Rossby and gravity modes as a function of a, y_o, α. Model results using a heat source centered at 11°S with an e-folding radius of 750 km and a time scale of about a day indicate that many aspects of the summertime upper tropospheric circulation over South America can be explained by the dispersive properties of Rossby and mixed Rossby–gravity waves. These results also show that the transient heat source excites Kelvin waves which propagate rapidly eastward as a nondispersive wave group. The existence of the Kelvin waves has implications for the initialization of tropical forecast models. By applying a nonlinear normal mode initialization procedure in the middle of a model simulation we investigate how the initialization distorts the subsequent evolution. Much of the distortion is associated with the Kelvin wave response.

Generaliza el modelo de Gill (lineal)

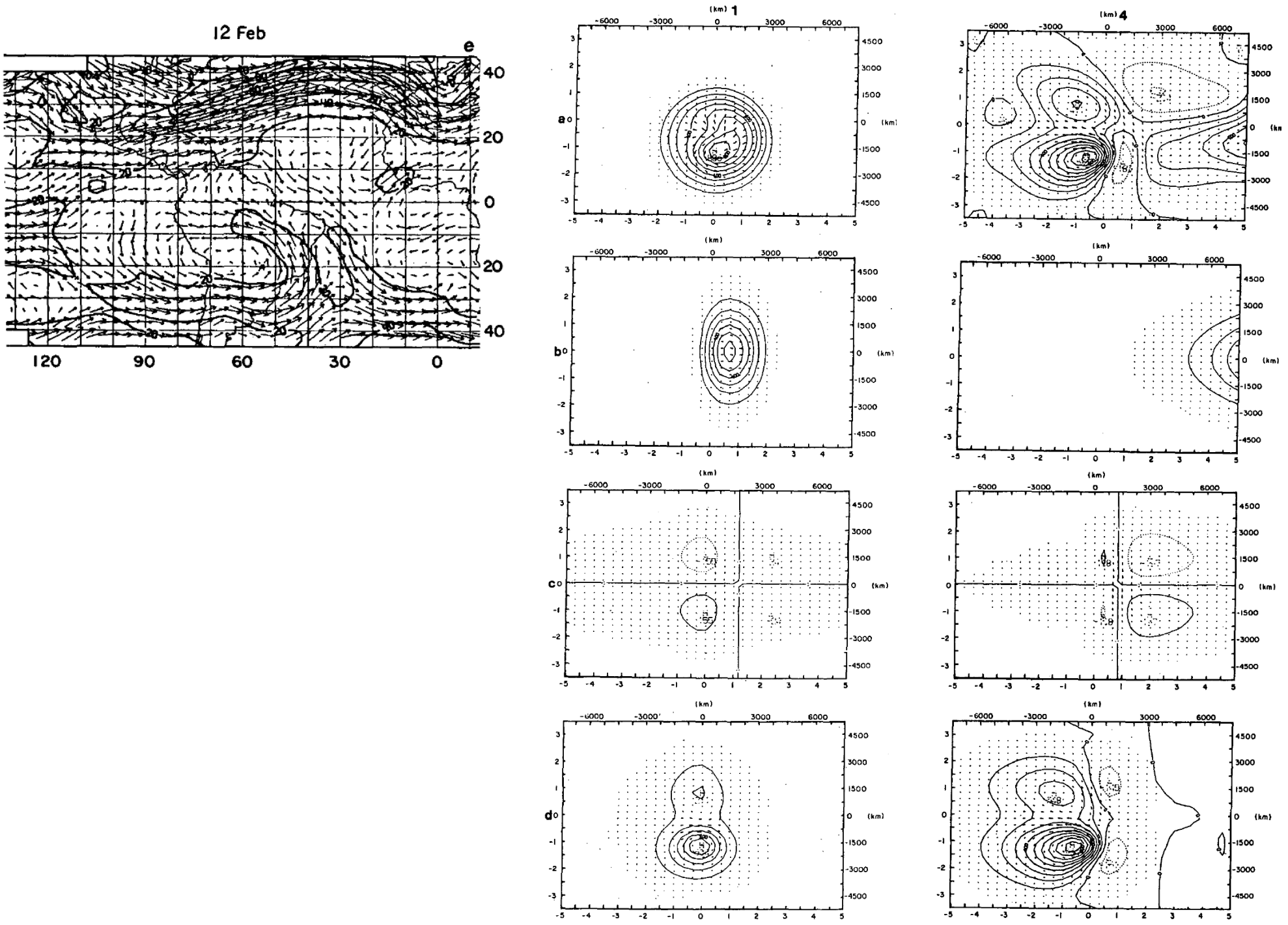

FIG. 4. Horizontal structure of the wind and geopotential fields at t = 16, 32, 48 and 64 h (columns 1, 2, 3 and 4, respectively) for the case of a heat source centered at $y_0 = -1200$ km (11°S) with time constant $\alpha^{-1} = 6$ h and horizontal scale $a = 750$ km. The total field is shown in (a) and the contribution to the total field from the Kelvin, mixed Rossby–gravity and Rossby waves are shown in (b), (c) and (d), respectively.

JOURNAL OF GEOPHYSICAL RESEARCH, VOL. 103, NO. D6, PAGES 6001–6015, MARCH 27, 1998

Impact of tropical heat sources on the South American tropospheric upper circulation and subsidence

Adilson W. Gandu and Pedro L. Silva Dias

Department of Atmospheric Sciences, Institute of Astronomy and Geophysics, University of Sao Paulo
Sao Paulo, Brazil

Abstract. The nonlinear adjustment of the wind and mass fields to idealized tropical heat sources is studied with a simple nonlinear primitive equation model with emphasis on the upper level circulation over South America and neighboring oceanic regions during the austral summer. Numerical experiments are performed with (1) an idealized symmetrical heat source in the Amazon region, (2) the asymmetry induced in source (1) by the SACZ, (3) the effect of the Atlantic ITCZ off the Amazon mouth, (4) the African heat source, (5) the West Pacific source, and (6) the central Pacific source during the warm phase of ENSO. The linear response is obtained through the reduction of the heat source by a factor of 10 and subsequent multiplication of the results by the same factor. Two basic questions are discussed: (1) are localized heat sources important for the development of the observed cyclonic flow in the midequatorial Atlantic and (2) where is the compensating subsidence associated with the Amazon heat source located? The nonlinearity helps organizing a weak cyclonic curvature in the midequatorial Atlantic, with the inclusion of source (2). The basic state generated by the west Pacific source, and primarily by the central Pacific source, has a large impact on the cyclonic curvature on the equatorial Atlantic. The compensating subsidence associated with the Amazon source is concentrated on the southwest side of the source. The SACZ extension helps to enhance the subsidence over the northern Argentina, and the Atlantic ITCZ enhances the subsidence over northeast Brazil and central equatorial Atlantic. Nonlinearity weakens the subsidence at the 500 hPa level inducing a more barotropic structure in the dynamical response to the heating.

Fuentes de calor idealizadas incluidas en modelo (no lineal)

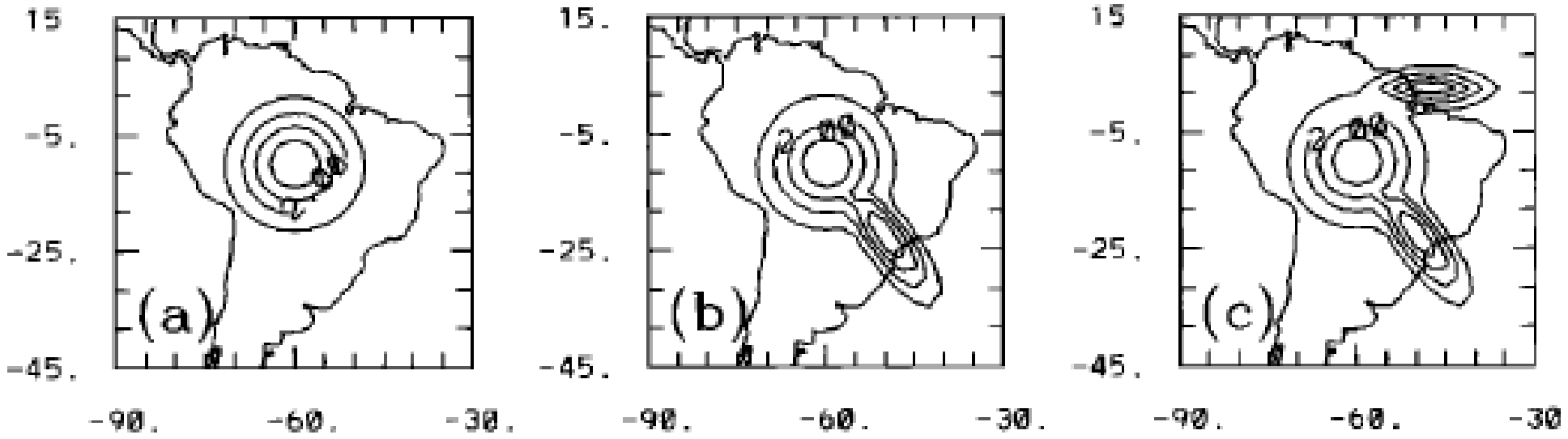

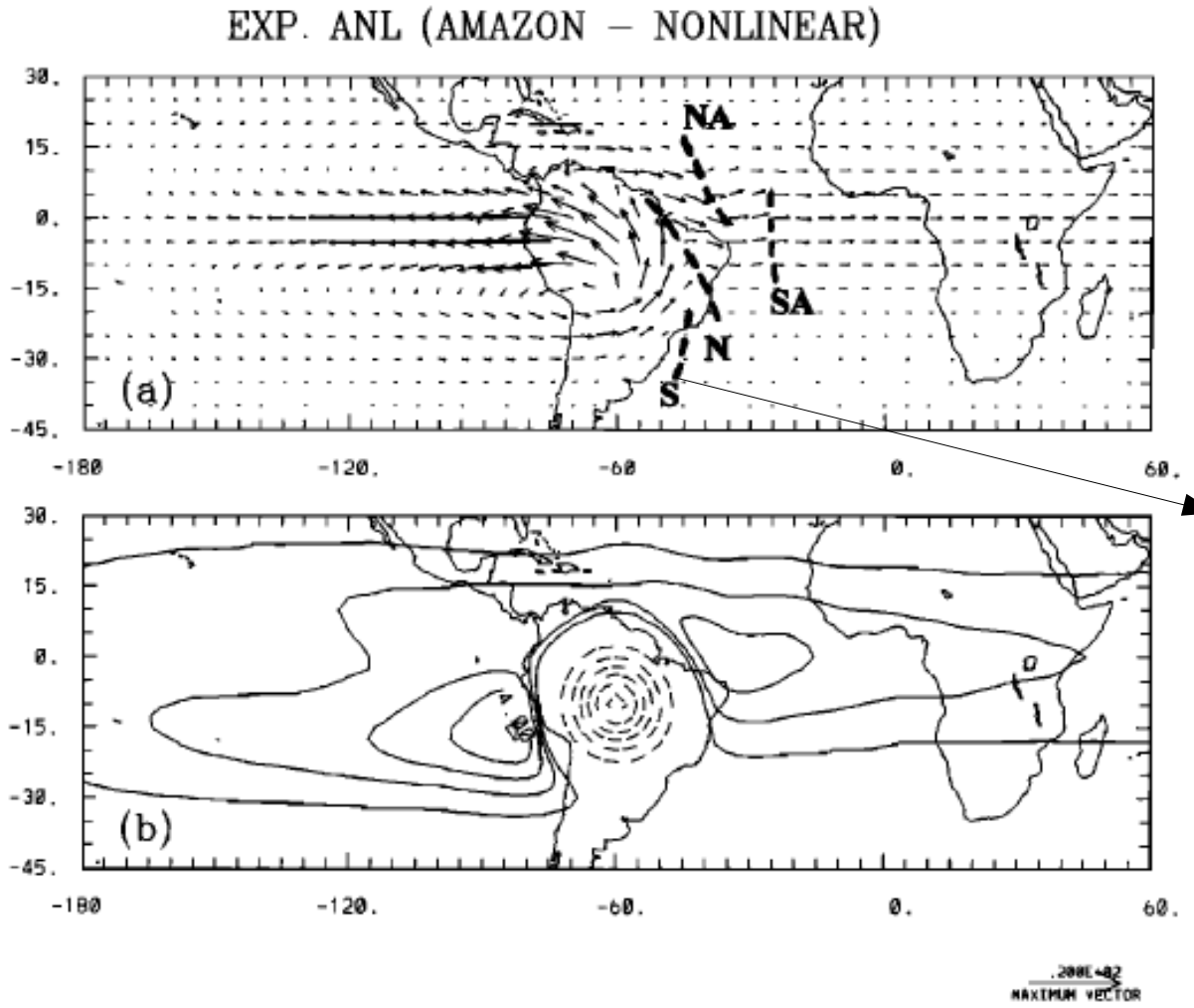

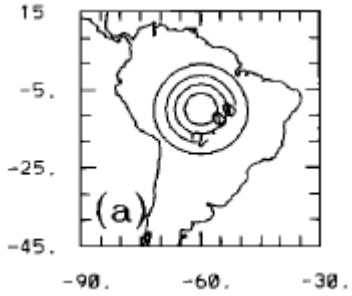

Vaguada: en lugar de SACZ => La posicion de la SACZ depende de la respuesta atmosferica a la conveccion en la Amazonas (Figueroa et al 1995)

Otra fuente de vorticidad ciclonica en la SACZ viene del Pacifico (Gandu SD 1995)

Figure 4. (a) The 200 hPa wind associated with the stationary response to experiment ANL (symmetric heat source over tropical South America) and (b) vertical motion in hPa/d at 500 hPa (contours are 20 hPa/d when $\omega < 0$ and 1 hPa/d when $\omega > 0$).

Gandu & Silva Dias 1998

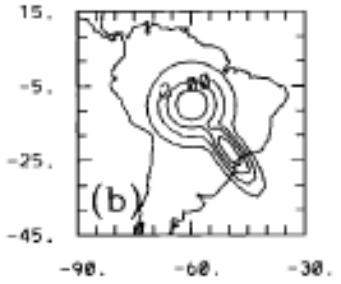

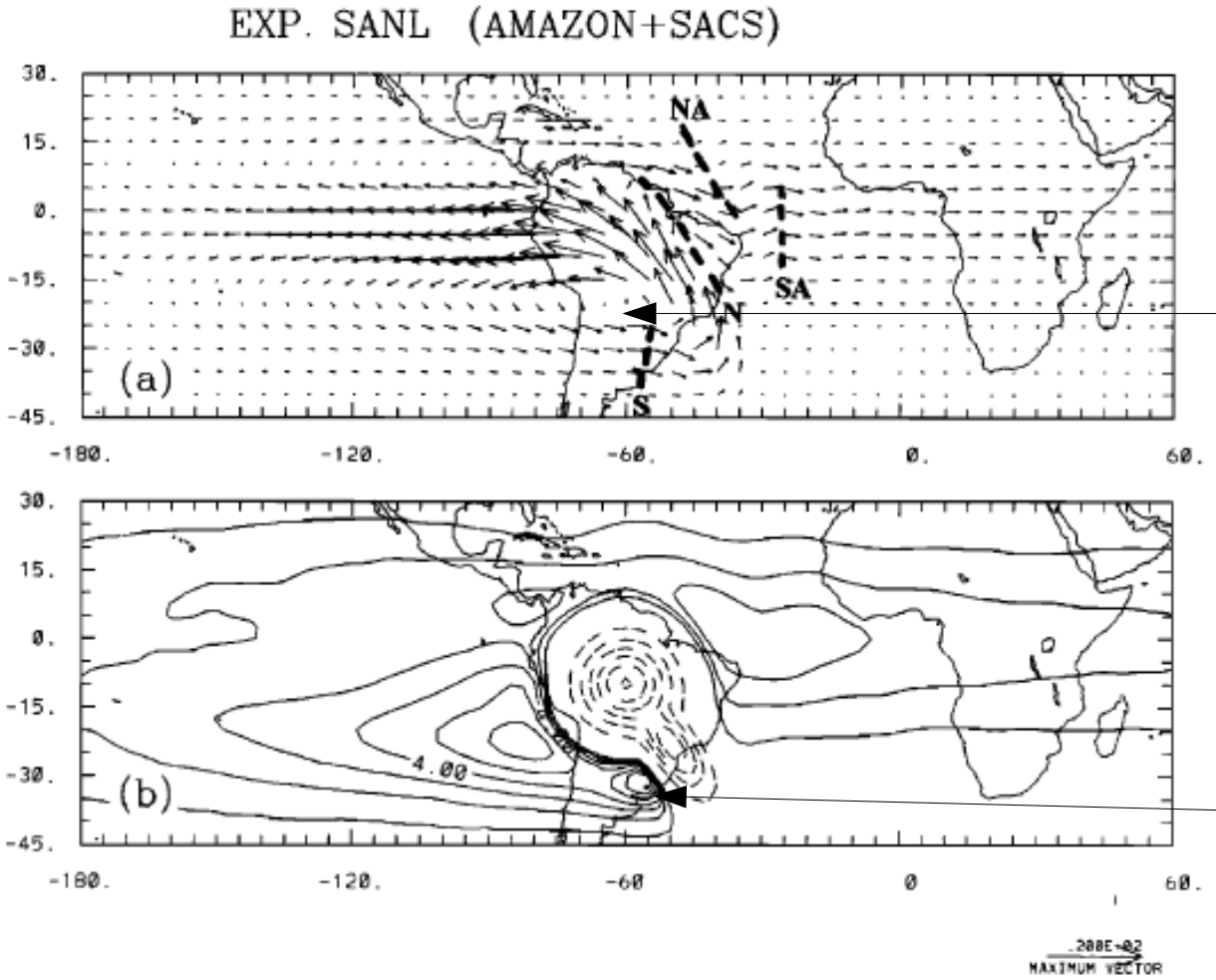

Figure 9. Same as Figure 4 but for experiment SANL (Amazon/central Brazil symmetric heat source and SACZ source).

Cuando la SACZ esta activa la Alta Boliviana se mueve al sureste.

La subsidencia compensatoria se encuentra al suroeste de la SACZ, sobre Uy.

Gandu & Silva Dias 1998

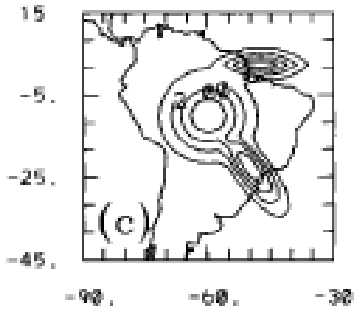

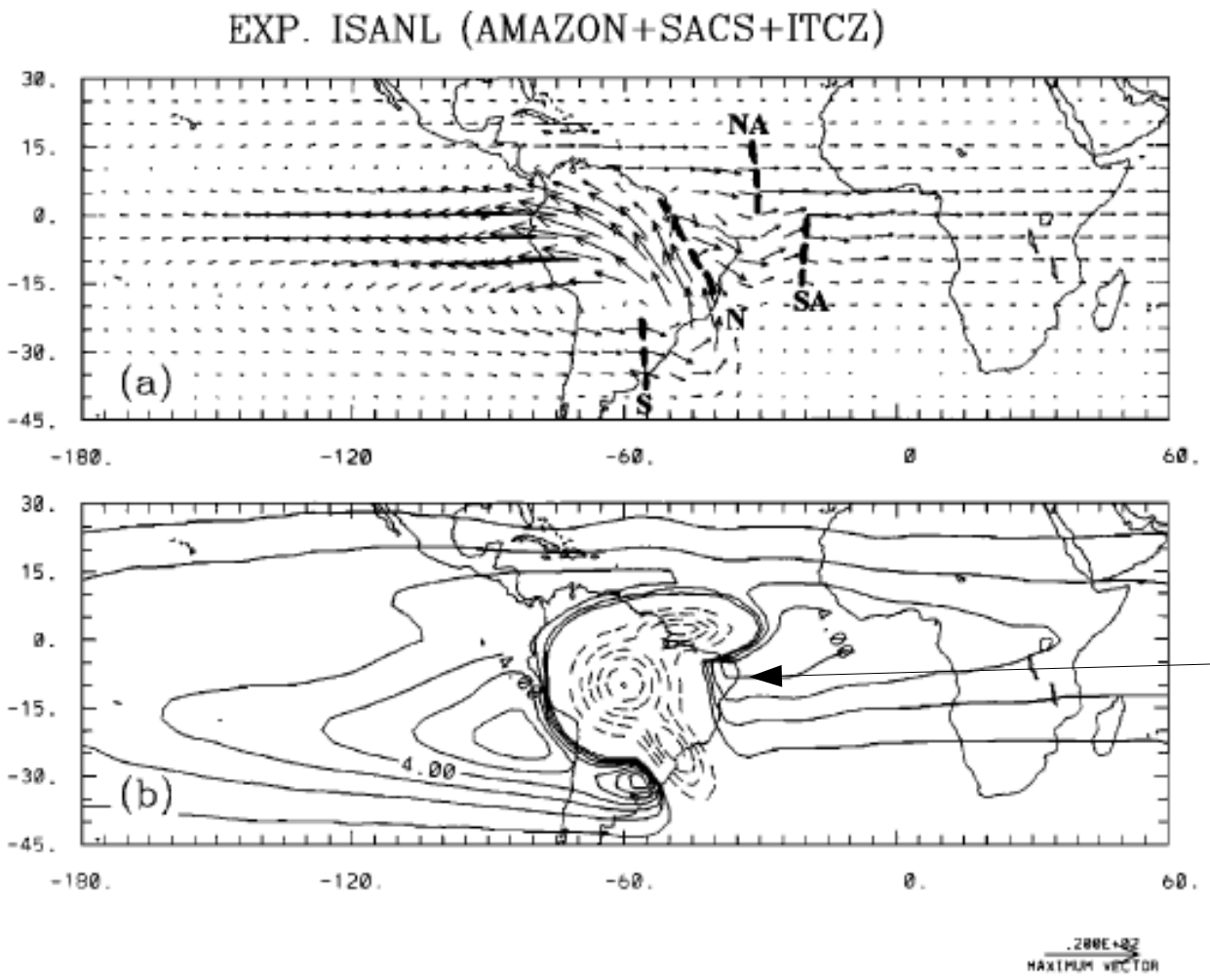

Mas subsidencia sobre el Nordeste de Brasil.

Figure 11. Same as Figure 4 but for experiment ISANL (Amazon/central Brazil heat source plus SACZ and Atlantic ITCZ sources).

Gandu & Silva Dias 1998

ZCAS activa

Vapor de agua

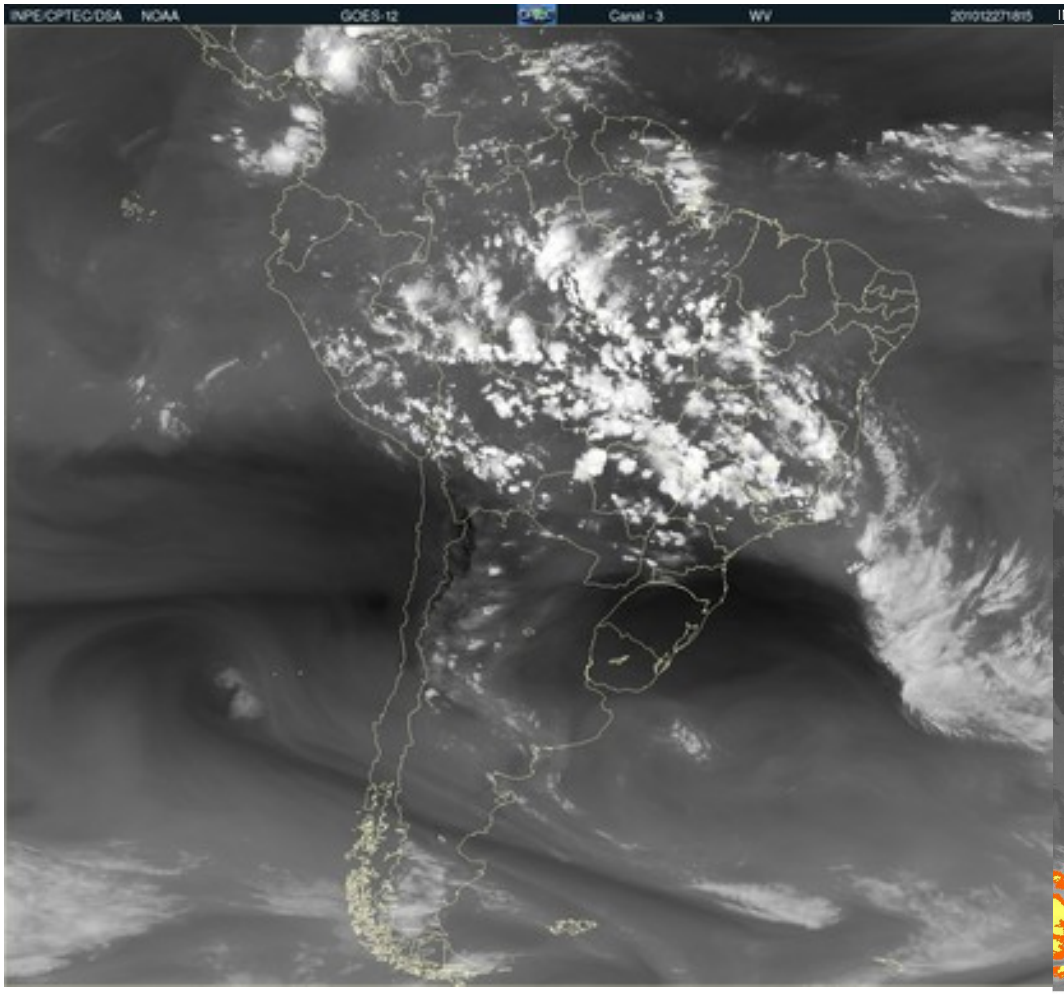

IR

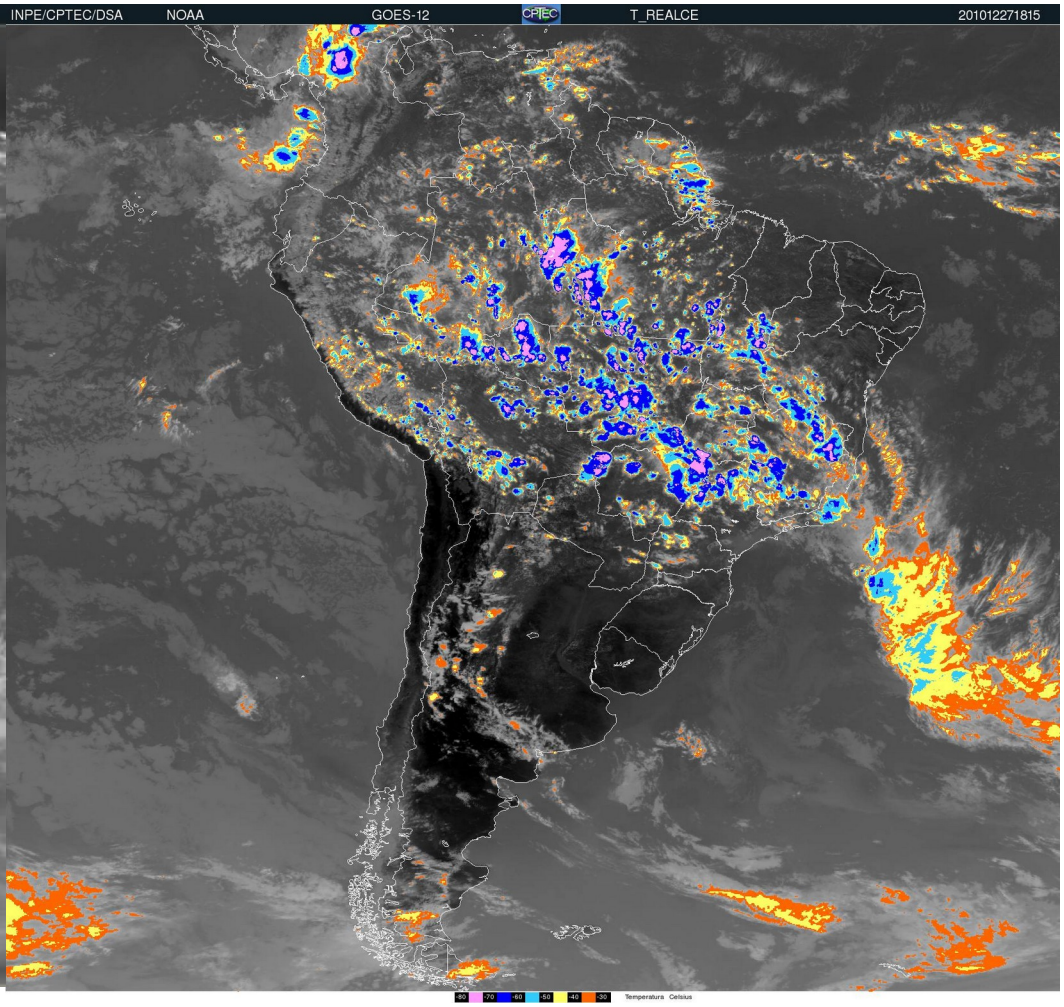

Otro día...

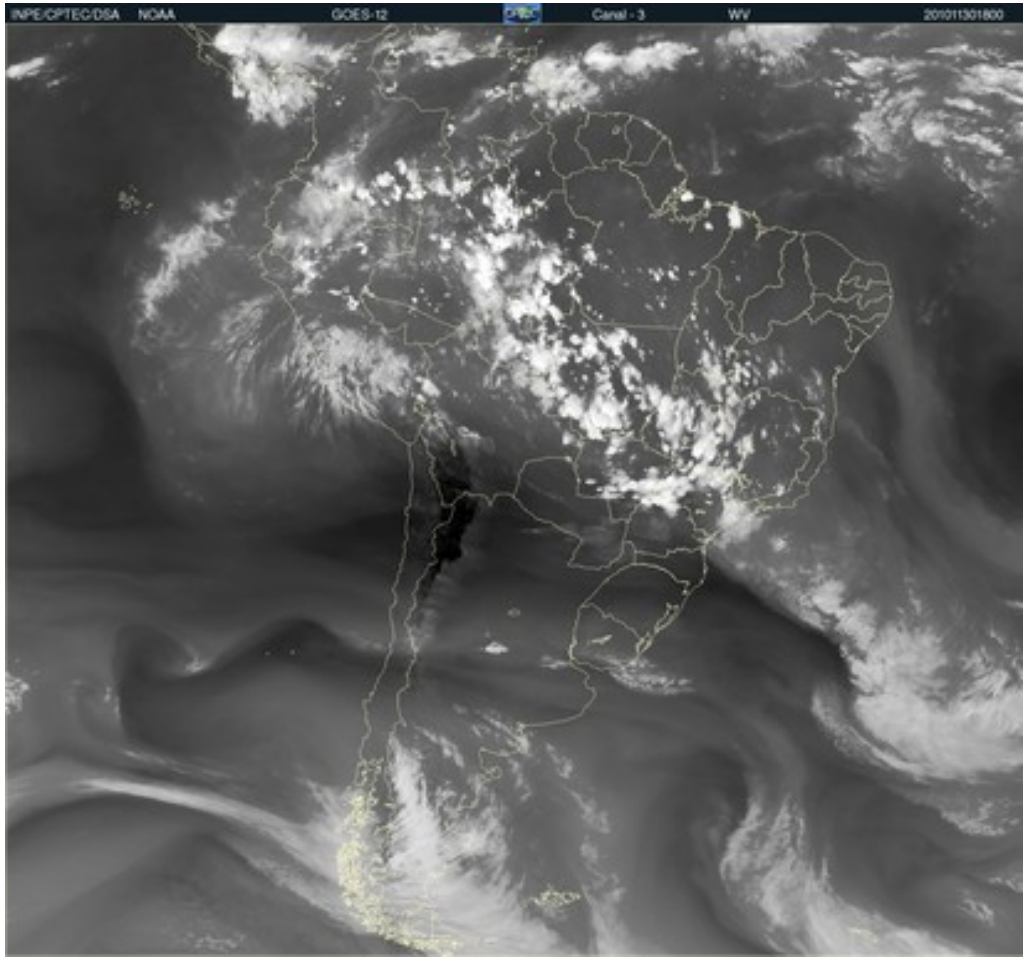
INPE/CPTEC/DSA NOAA GOES-12 Canal - 3 WV 201011301800

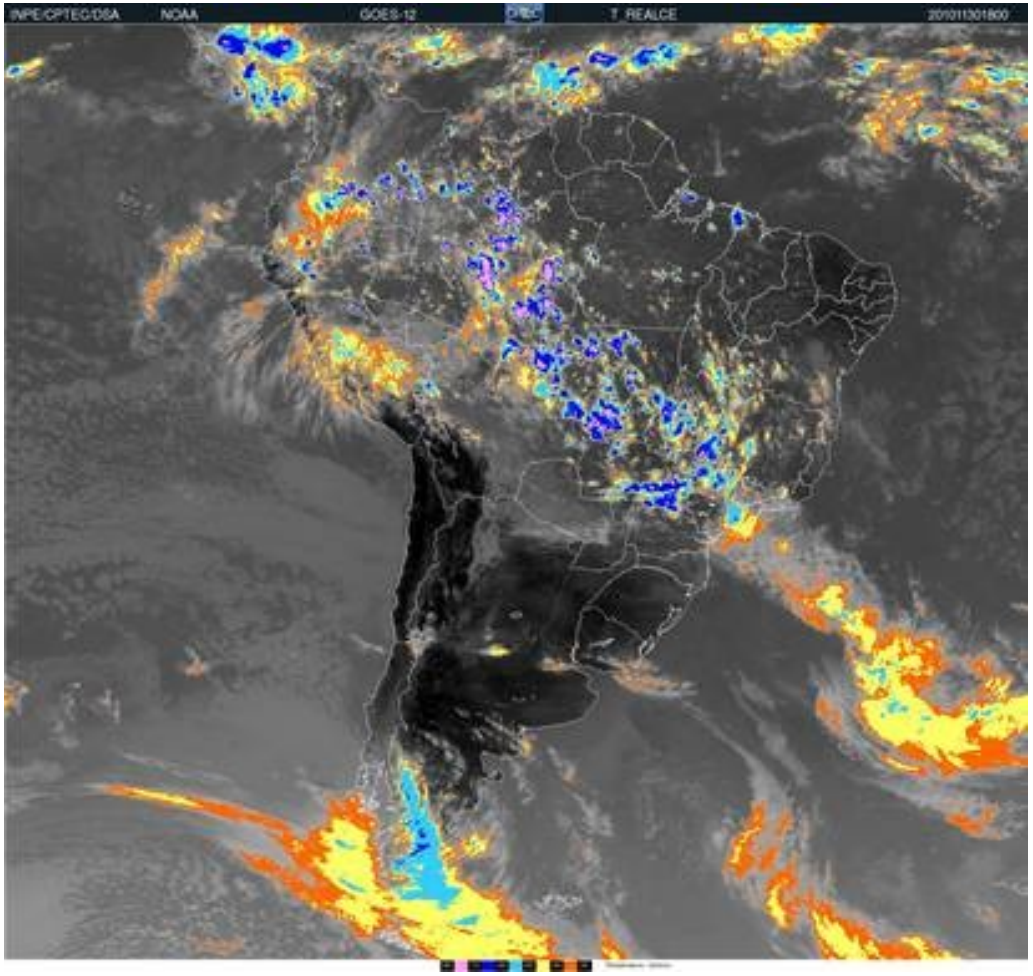
INPE/CPTEC/DSA NOAA GOES-12 T REALCE 201011301800

Otro día… 29/01/24

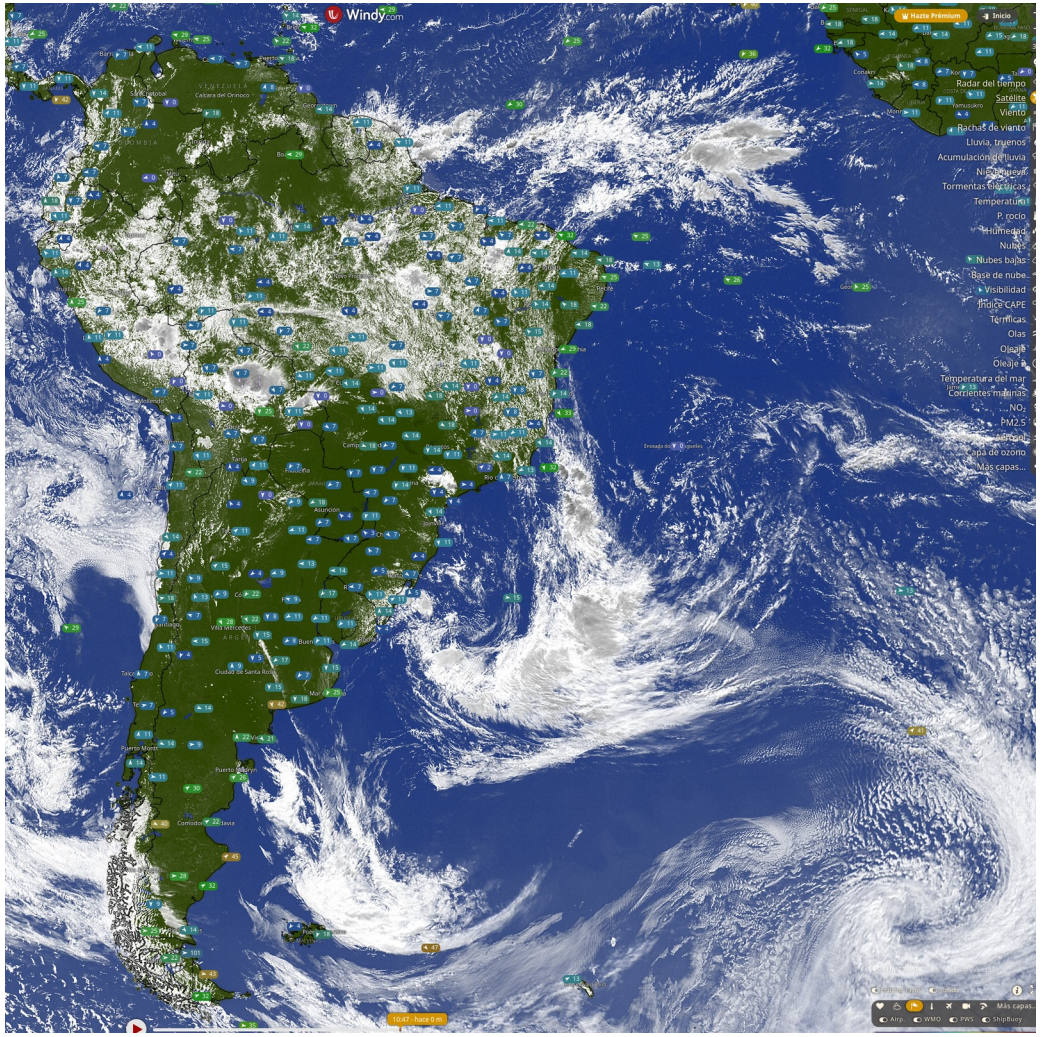

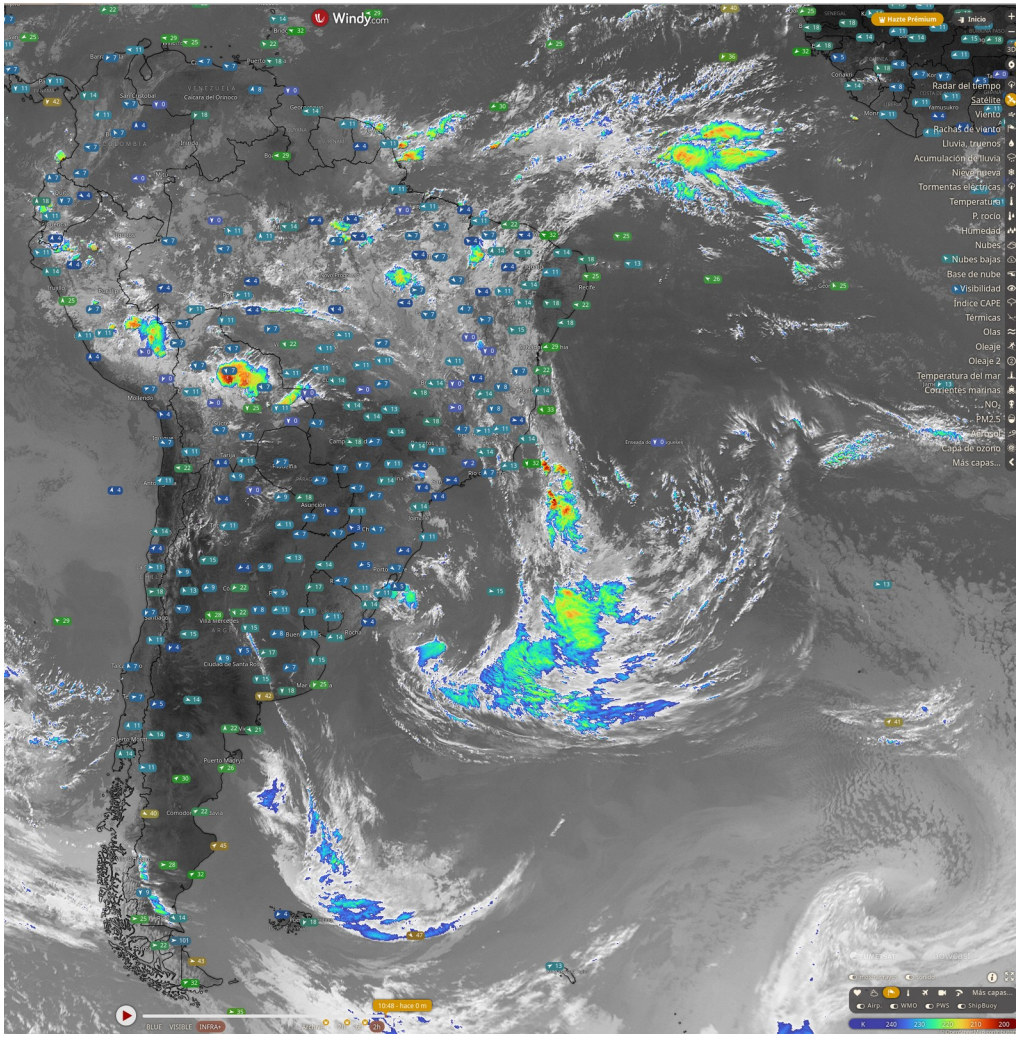

Configuración típica con SACZ activa (no mas de 10 días)

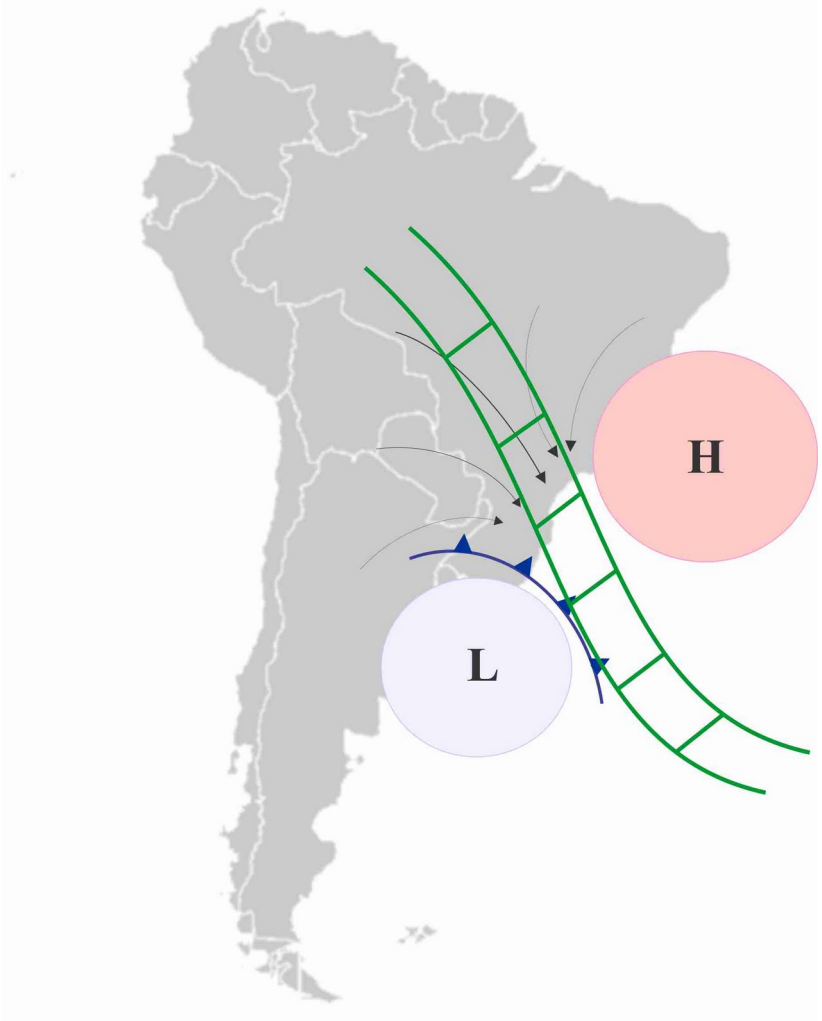

Typical positions of the SACZ (green) and the quasi-stationary surface frontal system (the low and the cold front), and convergence of low-level winds.

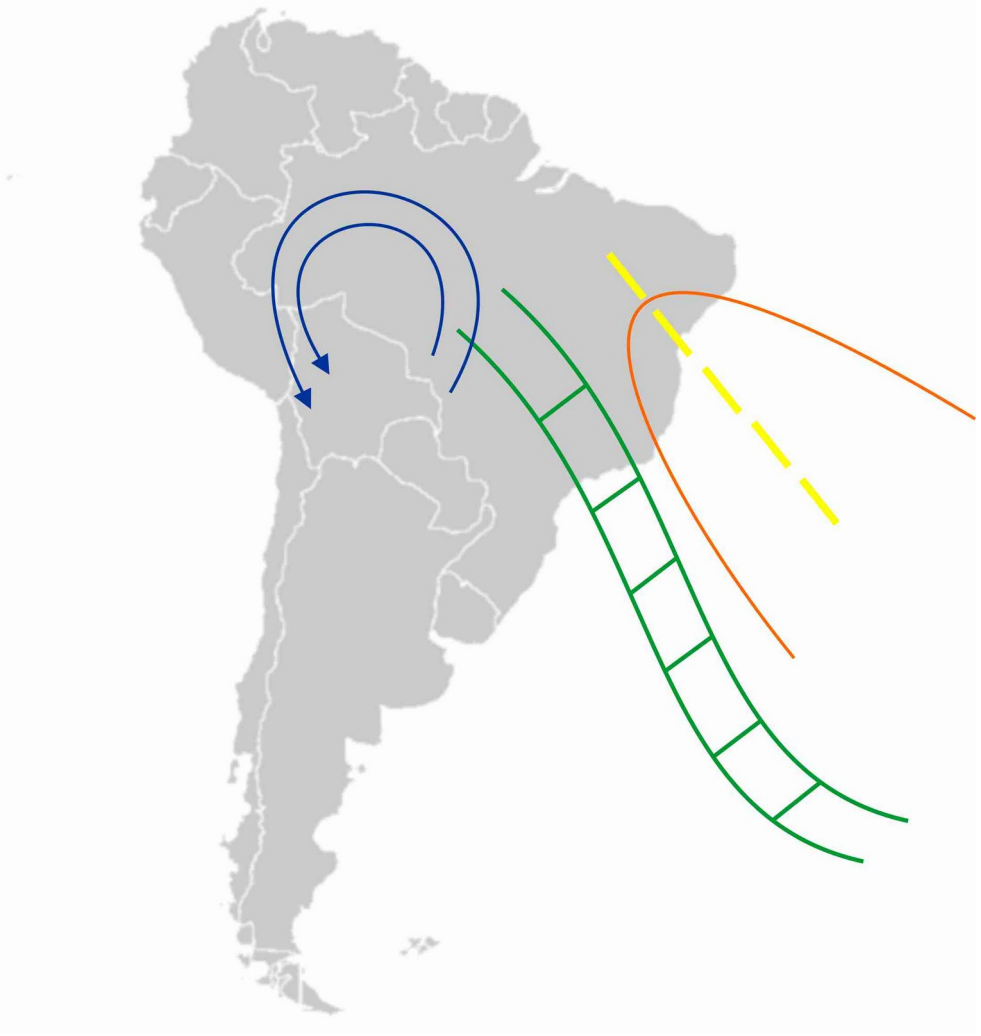

Typical configuration at high levels: an anticyclonic circulation (Bolivian high - blue lines) over northwestern South America and a trough over northeastern Brazil (orange and yellow lines).

https://resources.eumetrain.org/satmanu/CM4SH/Brazil/AtConZ/print.htm

La ZCAS es intensa cuando la convección en el Amazonas es intensa y está desplazada al sur de ecuador.

La ZCAS es robusta cuando los frentes penetran en los subtrópicos y se vuelven estacionarios cuando cruzan al este de la longitud de la convección Amazónica.

Este escenario es consistente con la observacion de que la ZCAS se forma luego del comienzo del monsón de AS.

Nieto Ferreira & Chao 2012

Variabilidad de ZCAS

- Escala Sinóptica- asociada a la penetración de frentes fríos
- Escala Subestacional- 10-100 días

  Máxima varianza en la ZCAS y región central de Am.Sur. Mínima varianza en Amazonia.

  Espectro muestra picos de 50, 27, 16, 10 y 8 días.

  → Asociado a MJO en banda 30-60 dias

  → Asociado a trenes de onda de latitudes medias en banda 2-30 dias, que estan a su vez asociados a MJO y ZCPS.

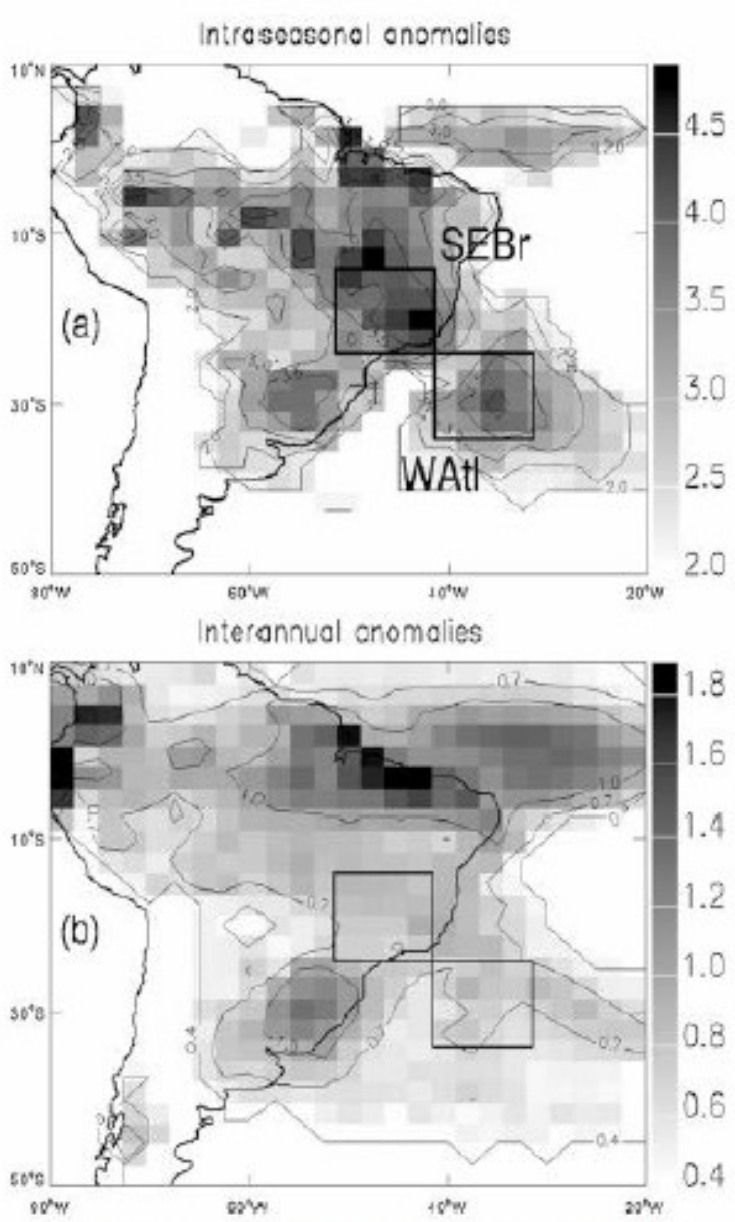

FIG. 2. (a) Intraseasonal (interval 2–5 mm day^{-1}) and (b) low-frequency (interval 0.4–1 mm day^{-1}) standard deviation of precipitation (shaded) (mm day^{-1}). The reference regions for composites are indicated by boxes.

La variabilidad intraestacional de la SACZ es mucho mayor que la Interanual.

Sobre Uy la variabilidad interanual es comparable a la intra-estacional

VARIABILIDAD INTRA-ESTACIONAL

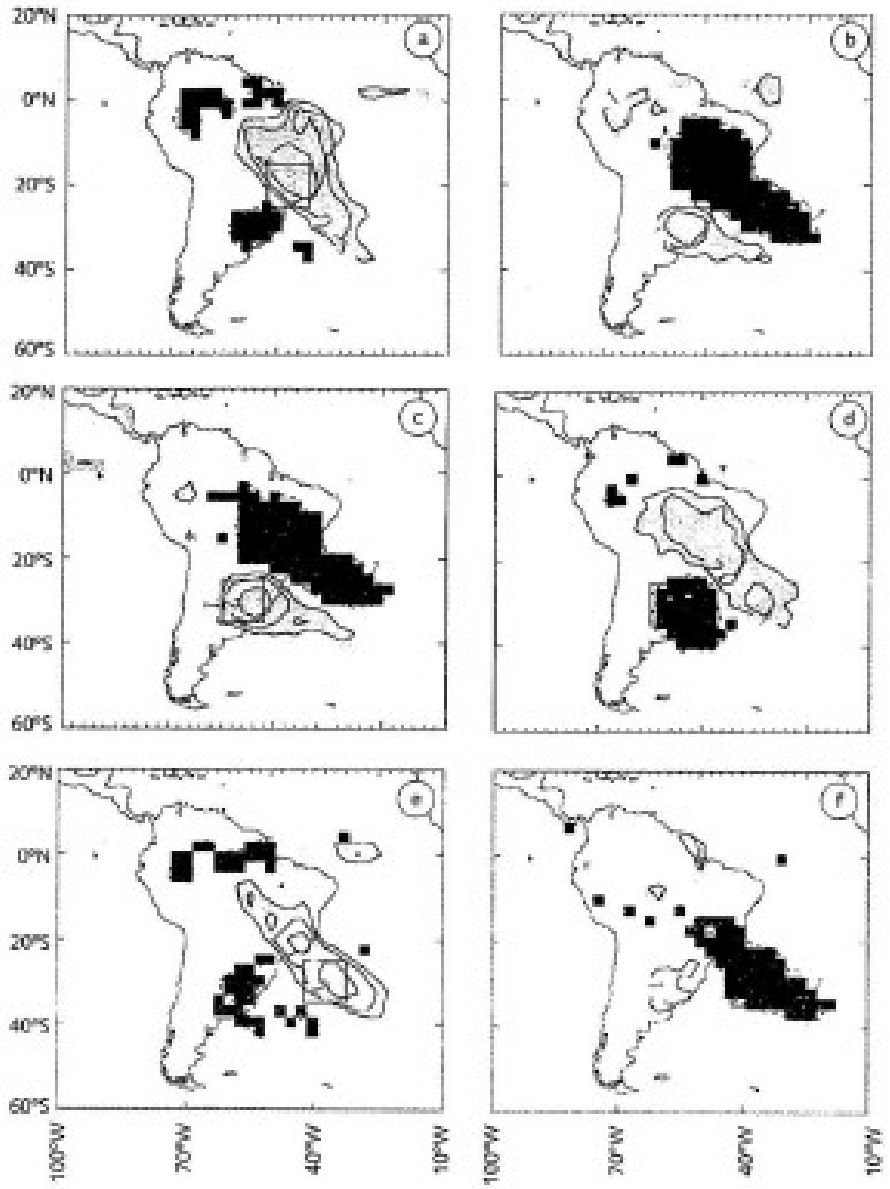

FIG. 6.4 Composições de anomalias intrassazonais de precipitação (20-90 dias) derivadas de Global Precipitation Climatology Project (GPCP) (mm/dia). A coluna da esquerda (direita) é para composições de eventos extremos úmidos (secos) em diferentes regiões: (a) e (b) no Sudeste do Brasil; (c) e (d) no Sul do Brasil; (e) e (f) no Atlântico Oeste. Primeiro contorno positivo (negativo) é de 1,0 (-1,0), com intervalo de 2,0 mm/dia. Regiões sombreadas indicam significância estatística de 95%
Fonte: Muza et al., 2009.

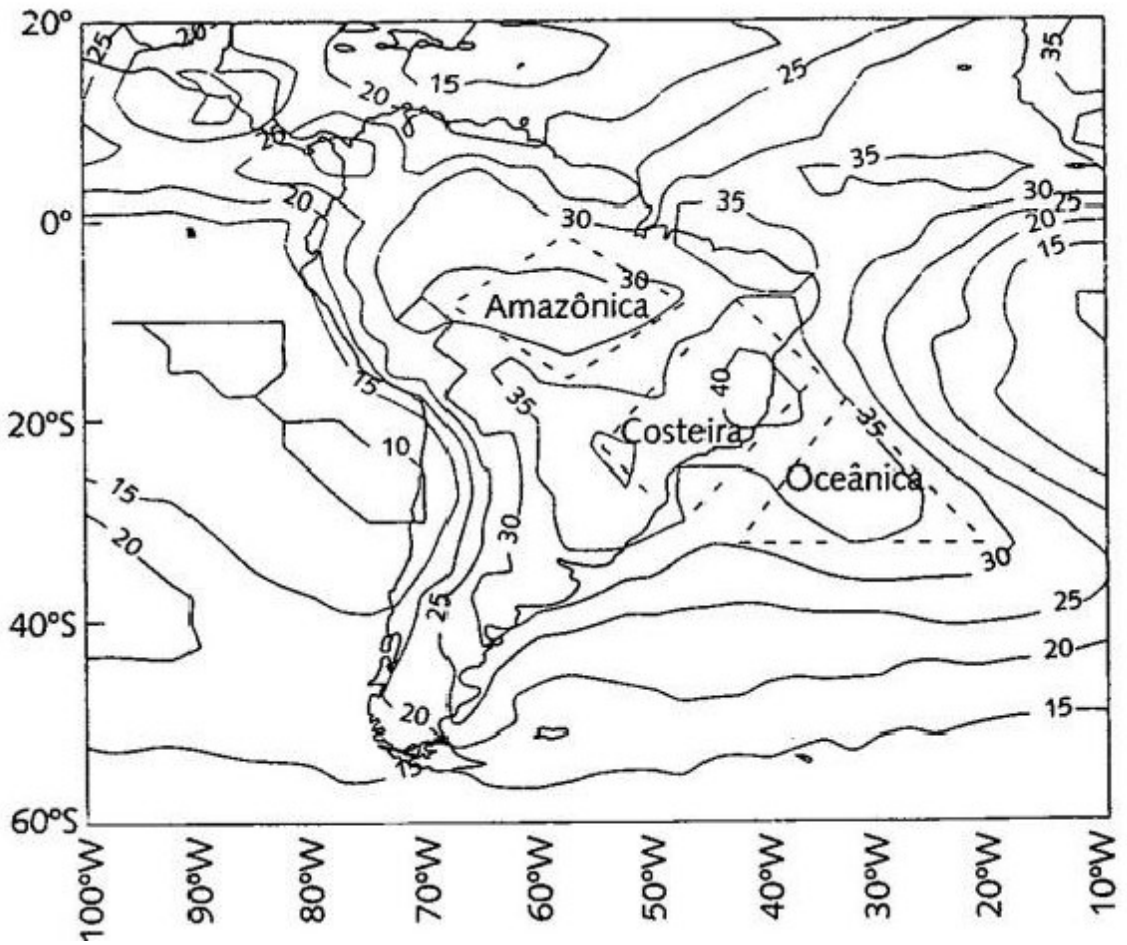

FIG. 6.2 Desvio padrão de ROL (W m^{-2}) durante os meses de dezembro, janeiro e fevereiro (1979-1996). Áreas indicadas em linhas tracejadas localizam as regiões com máximo desvio padrão em escalas subsazonais (costeira e oceânica) e máxima atividade convectiva em escalas subsazonais (amazônica). Ver Carvalho, Jones e Liebmann, 2004 para mais detalhes

EXAMPLE OF OLR_{200} PROPERTIES

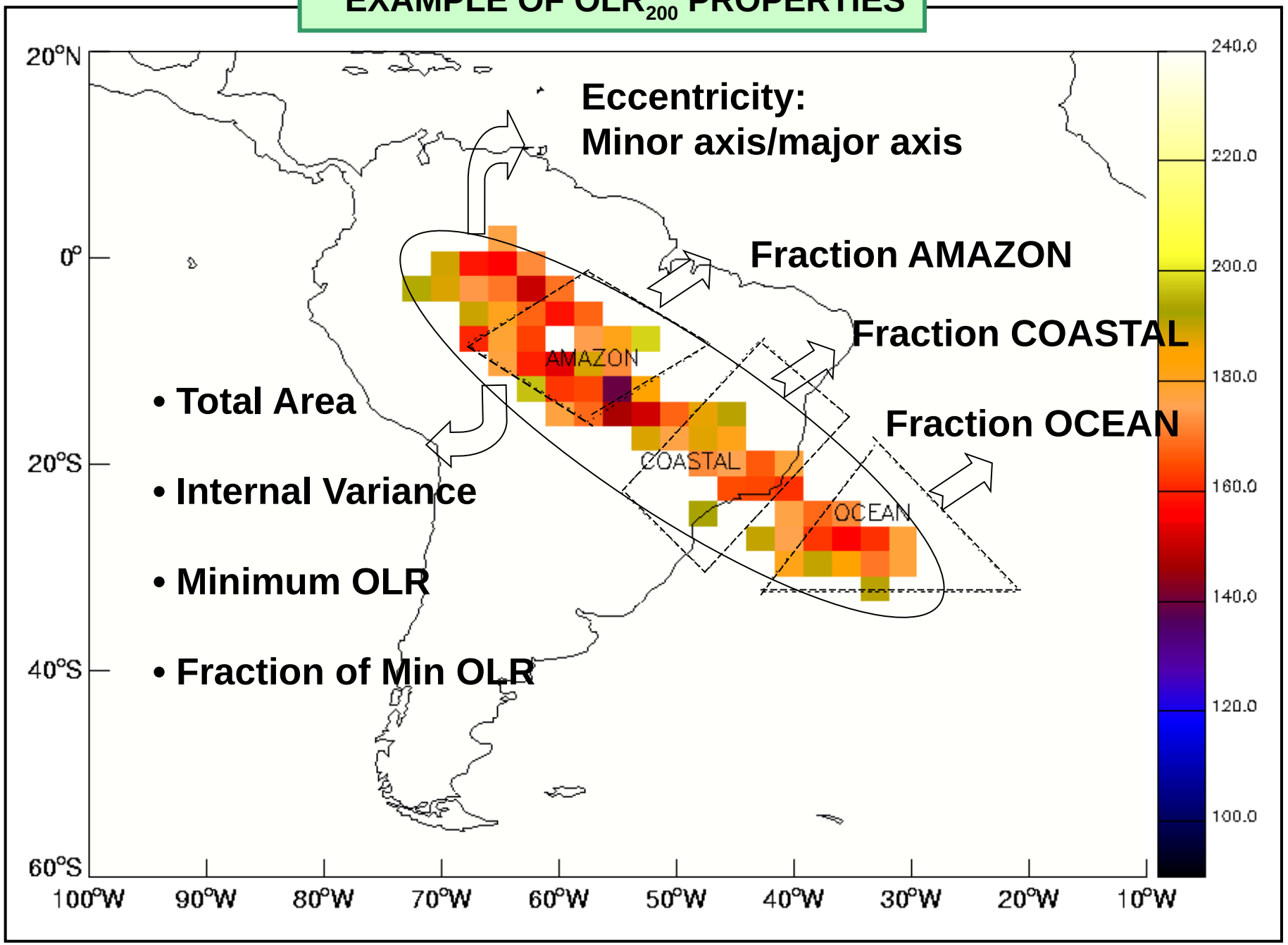

Carvalho et al 2002

OLR Daily Anomalies (W m^{-2}) Intense SACZ

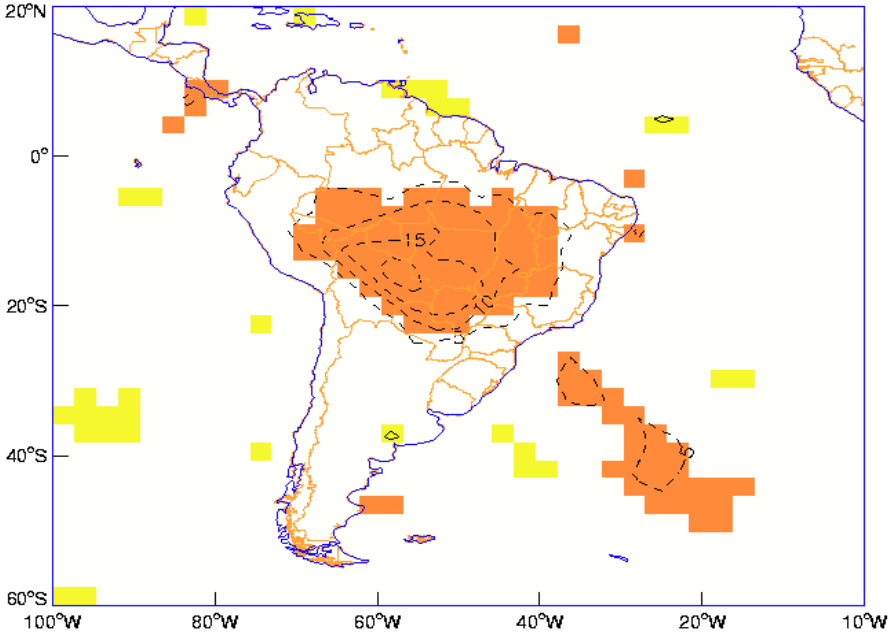

OLR Daily Anomalies (W m^{-2}) Weak SACZ

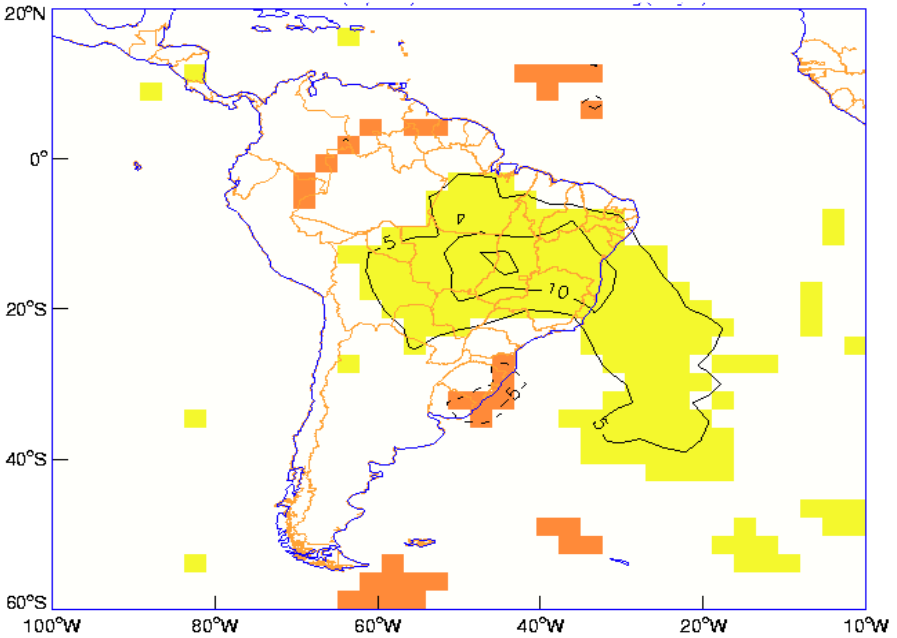

OLR Daily Anomalies (W m^{-2}) Oceanic SACZ

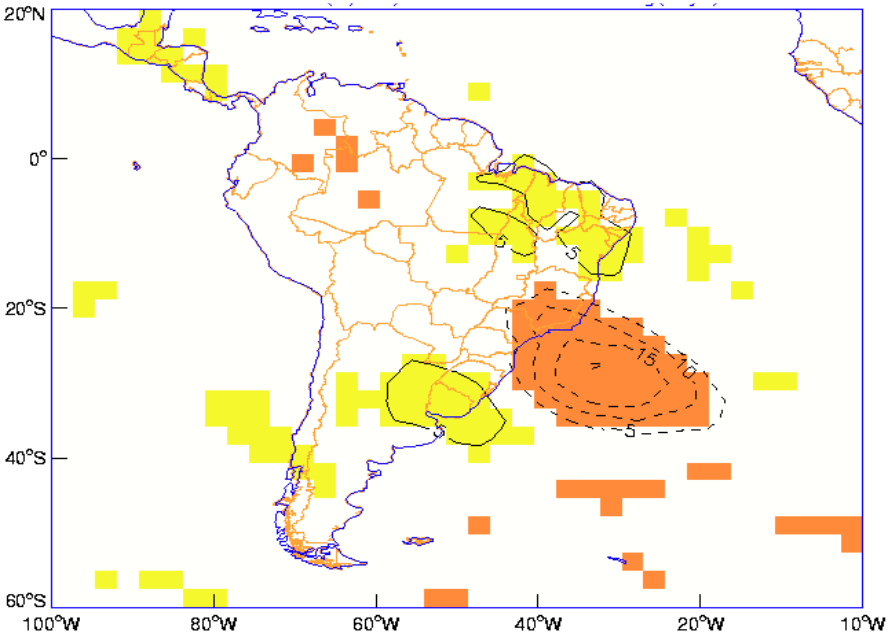

OLR Daily Anomalies (W m^{-2}) Continental SACZ

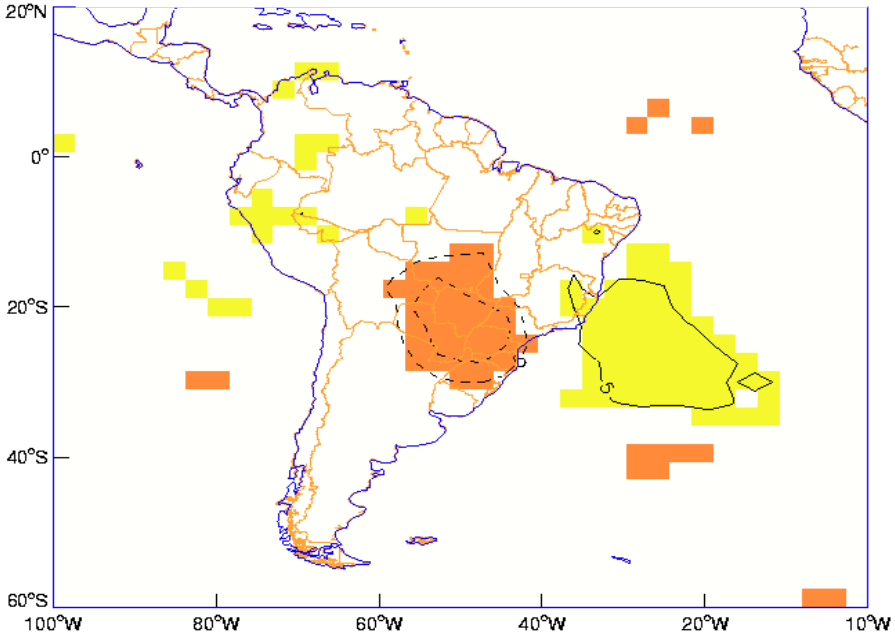

Figure 3

Las componente oceanica y continental de la SACZ son cuasi-independientes.

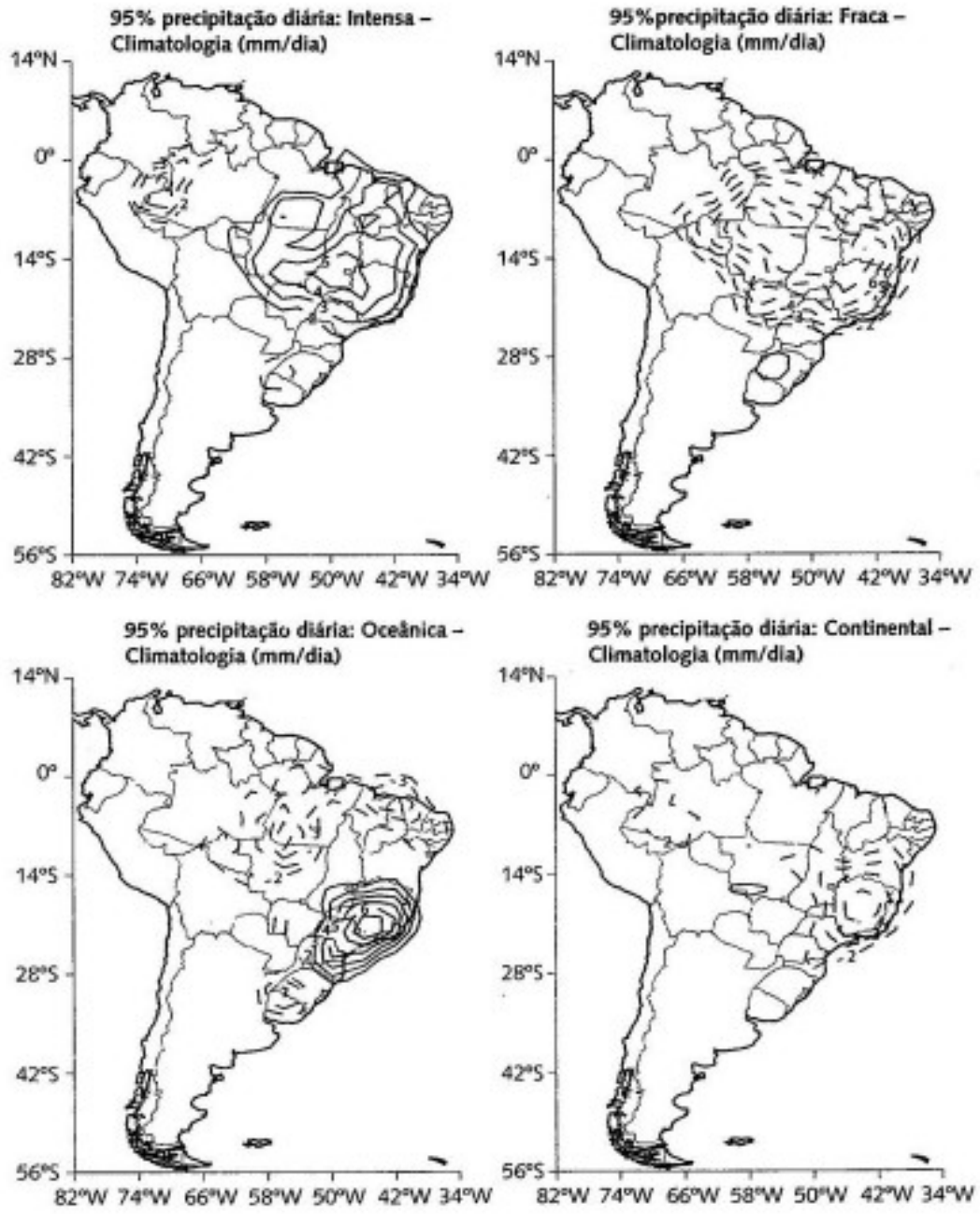

Fig. 6.6 Diferença entre o percentil de 95% na precipitação em diversas categorias de ZCAS e o percentil de 95% da precipitação na climatologia (dezembro a fevereiro). Linhas sólidas (tracejadas) indicam diferenças positivas (negativas) Fonte: Carvalho, Jones e Liebmann, 2004.

SACZ Composites 10-90 days anomalies Carvalho et al 2002

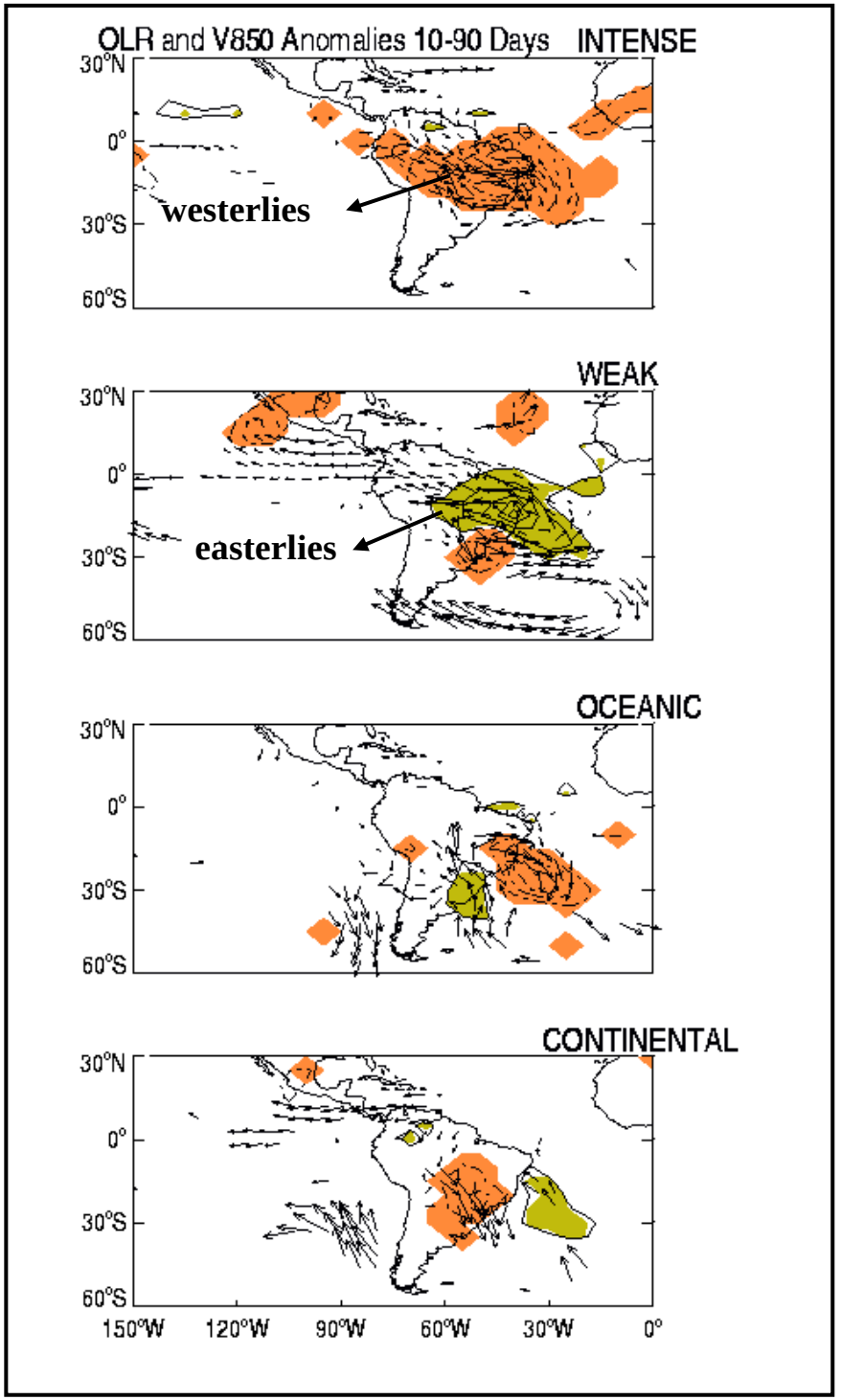

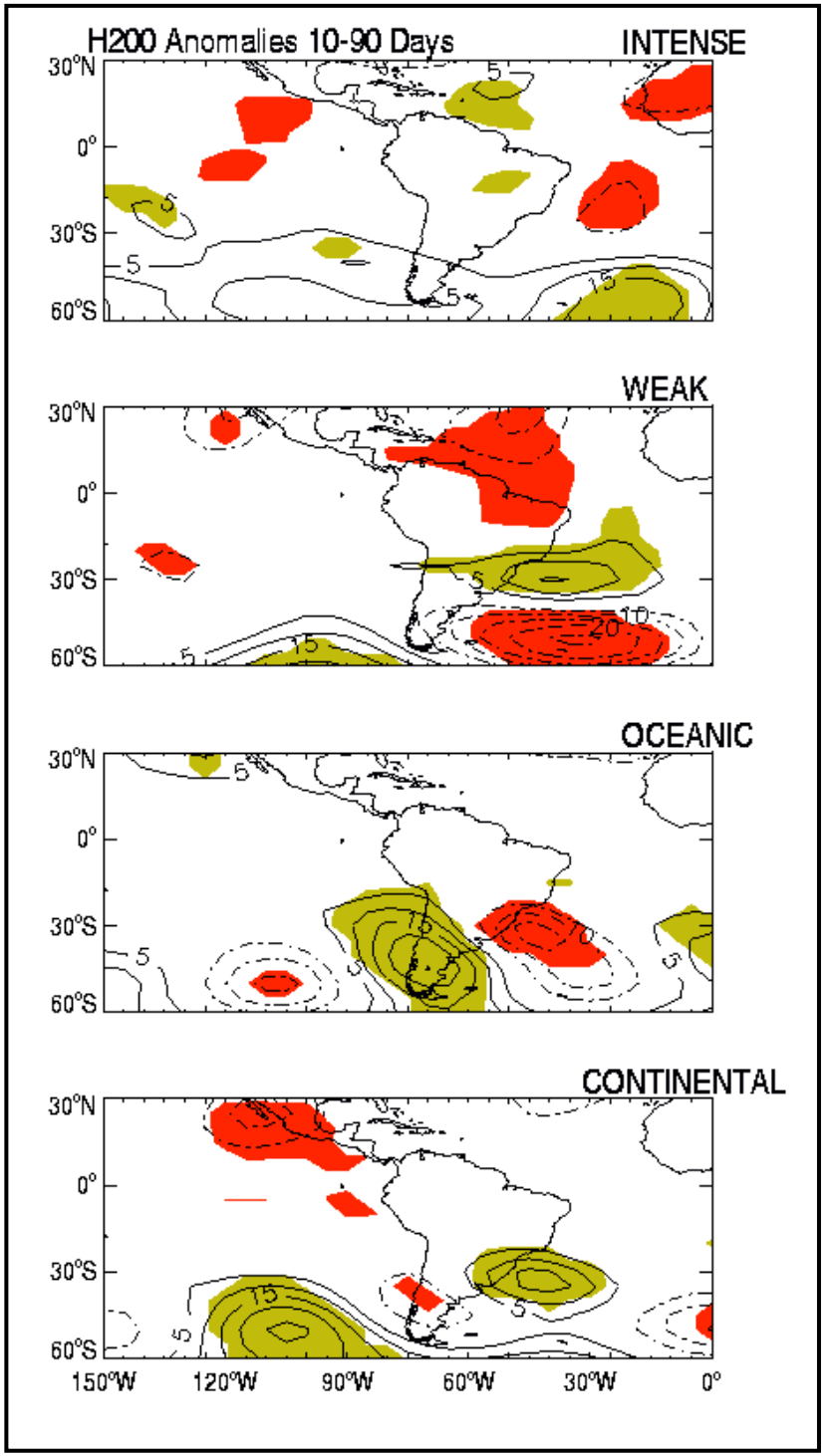

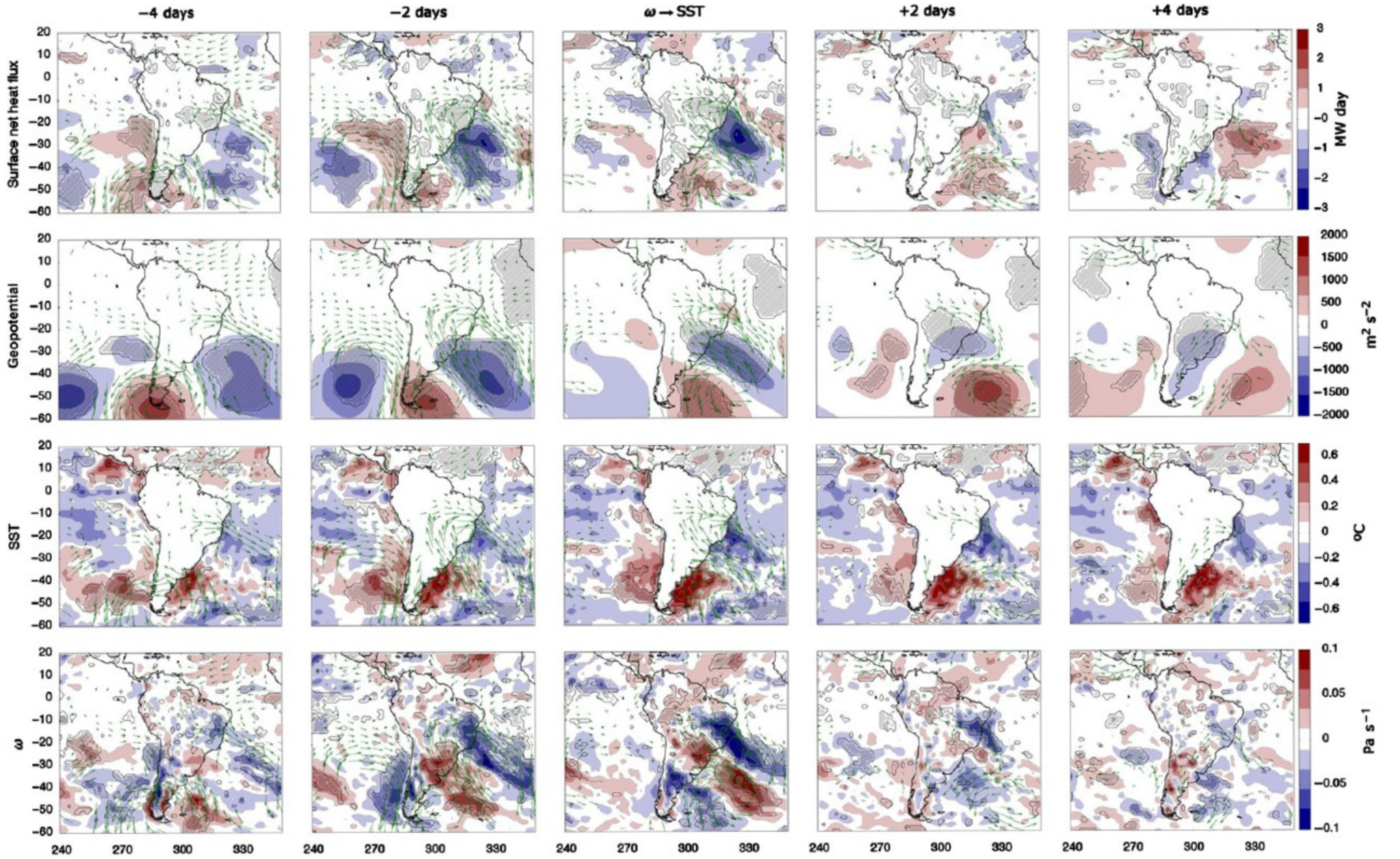

Figure 5. Lagged composites of ω anomalies at 500 hPa, SST anomalies, geopotential anomalies at 200 hPa and surface net heat flux anomalies for $\omega \rightarrow$ SST cases. Wind anomalies at 850 hPa are also included as vector field in all the maps. Black shading marks areas of 90% significance, moreover only arrows related to wind anomalies significant at 90% are reported.

Tirabassi et al 2014

Intraseasonal variability in South America

1st EOF leading pattern of 10-90-day filtered OLR variability

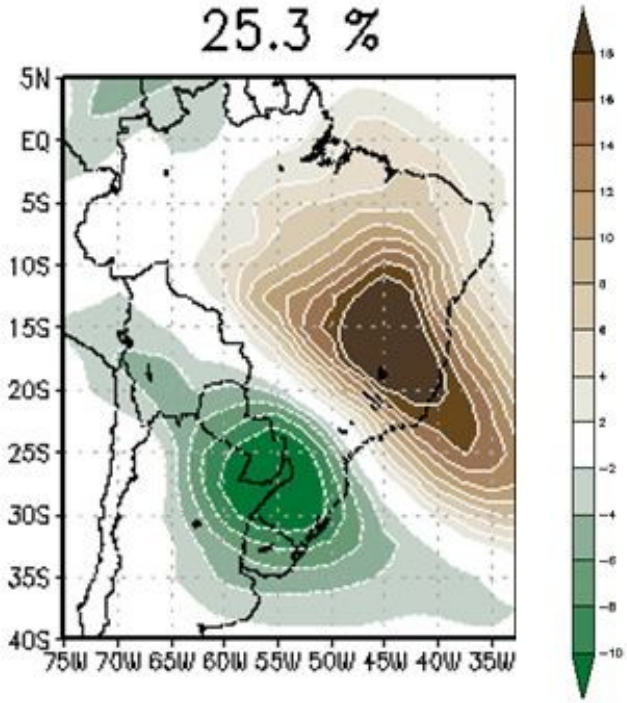

SOUTH AMERICAN SEE-SAW PATTERN

C I M A
CONICET
U B A

Weakened SACZ

Intensified SALLJ poleward progression

Higher frequency of extreme daily rainfall events at the subtropics

(Liebmann, Kiladis, Saulo, Vera, and Carvalho, 2004)

(Gonzalez, Vera, Liebmann, Kiladis, 2008)

Intensified SACZ

Inhibited SALLJ poleward progression

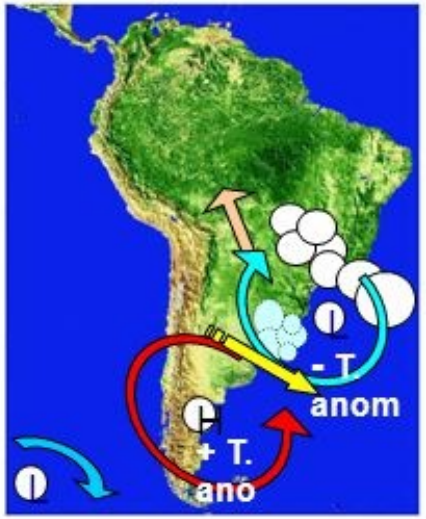

Higher frequency of heat waves and extreme daily temperature events at the subtropics

(Cerne , Vera, and Liebmann, 2007, Cerne and Vera, 2010)

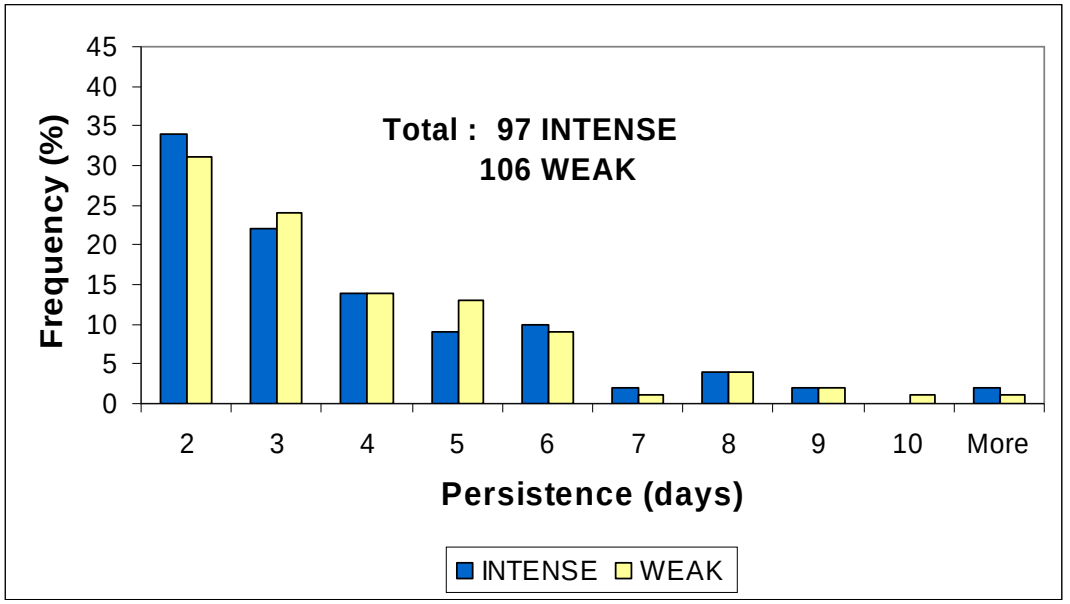
Frequency (%)
45
40
35
30
25
20
15
10
5
0
Total : 97 INTENSE
106 WEAK
2
3
4
5
6
7
8
9
10
More
Persistence (days)
INTENSE
WEAK

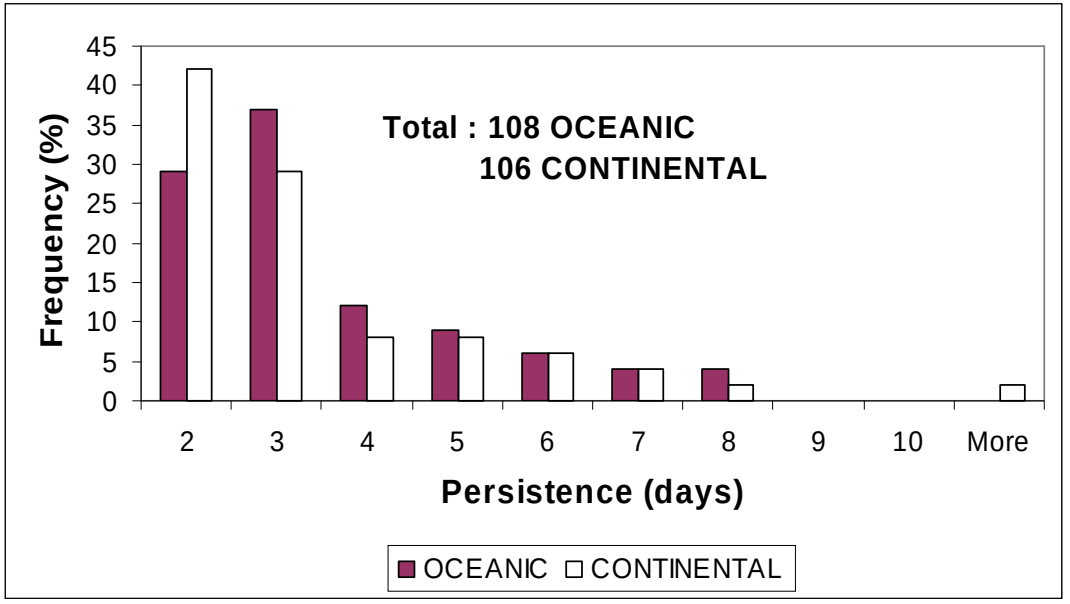
Frequency (%)
45
40
35
30
25
20
15
10
5
0
Total : 108 OCEANIC
106 CONTINENTAL
2
3
4
5
6
7
8
9
10
More
Persistence (days)
OCEANIC
CONTINENTAL

TIME-INTERVAL BETWEEN PERSISTENT EVENTS

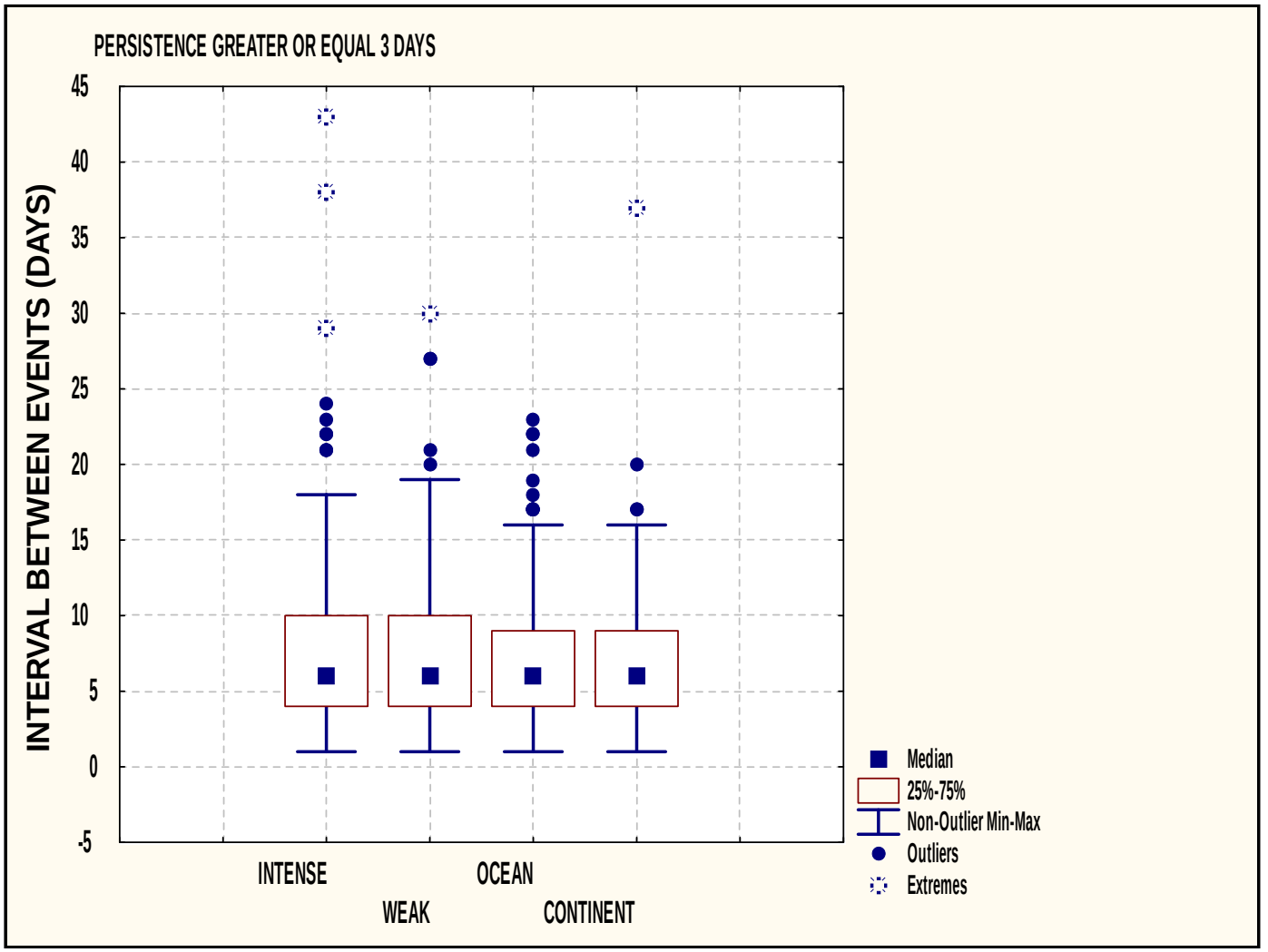

Outliers : data point values ≥ 1.5 times the interquartile range.
Extremes: data point values ≥ 3.0 times the interquartile range.

ZCAS y OMJ

- Diaz N., M. Barreiro, N. Rubido, 2022: The distinct influence of two Madden-Julian's trajectory classes on the South American Dipole. J. Climate doi.org/10.1175/JCLI-D-21-1001.1.
- Diaz N., M. Barreiro, N. Rubido, 2020: Intraseasonal Predictions for the South American Rainfall Dipole. Geophys. Res. Lett. doi.org/10.1029/2020GL089985.
- Barreiro M., L. Sitz, S. de Mello, R. Fuentes Franco, M. Renom, R. Farneti, 2019: Modeling the role of air-sea interaction in the impact of MJO on South American climate Int. J. Climatology, 39(2), 1104-1116.

1st EOF leading pattern of 10-90-day filtered OLR variability

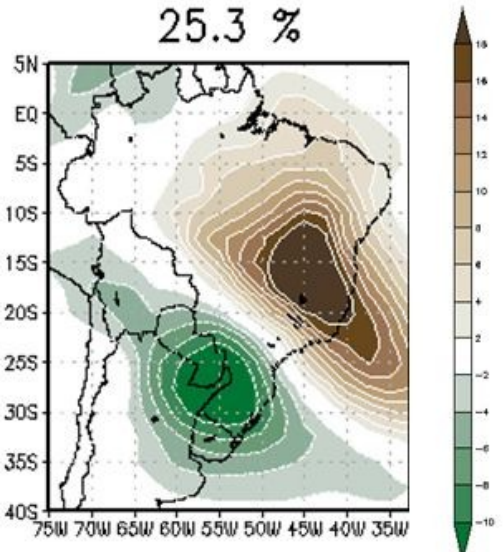

VARIABILIDAD INTERANUAL

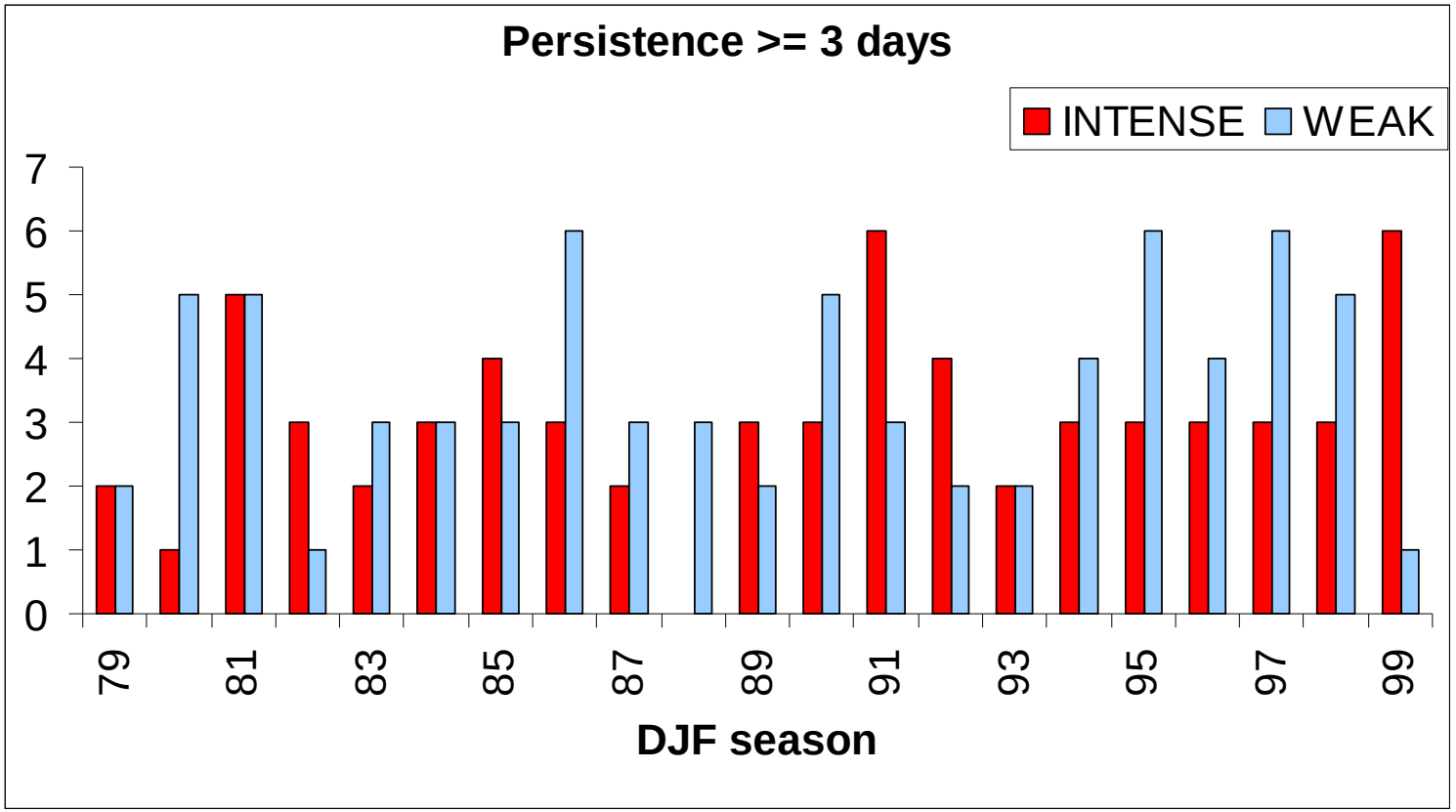

INTER-ANUAL

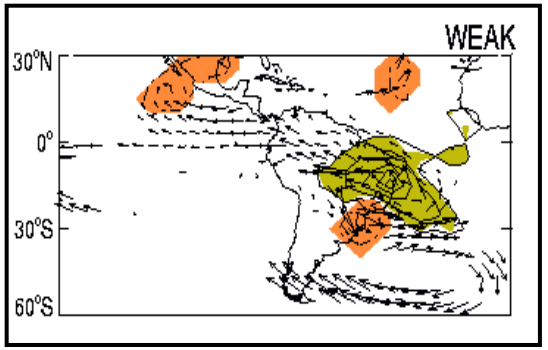

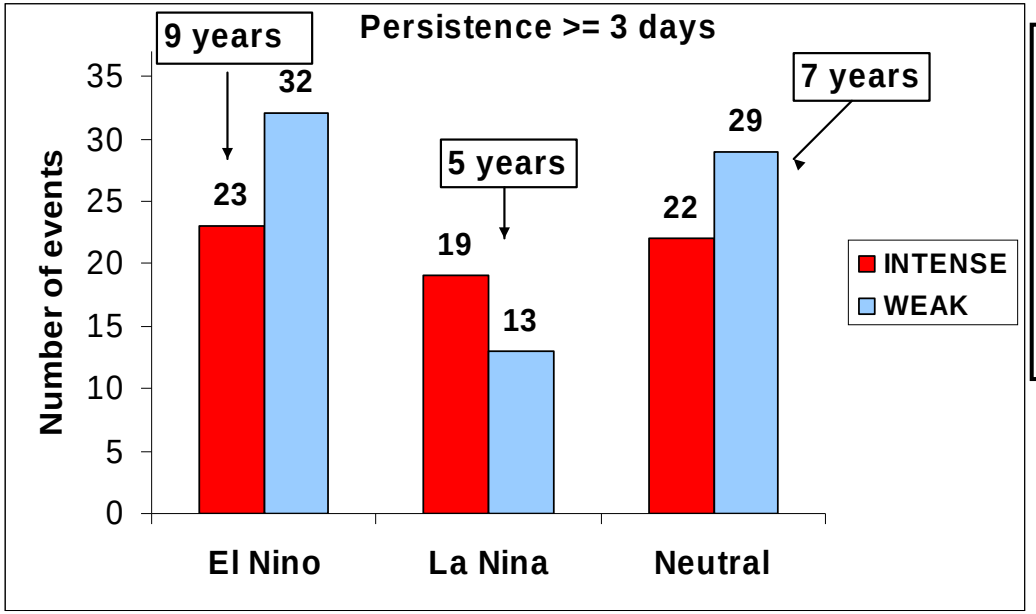

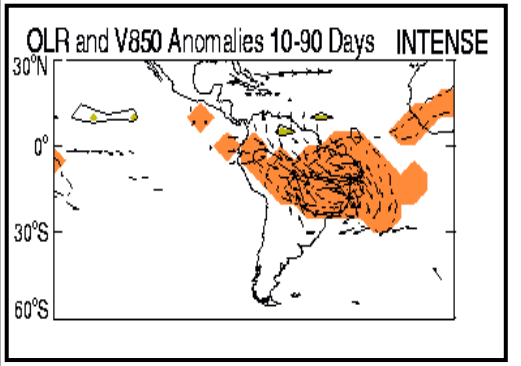

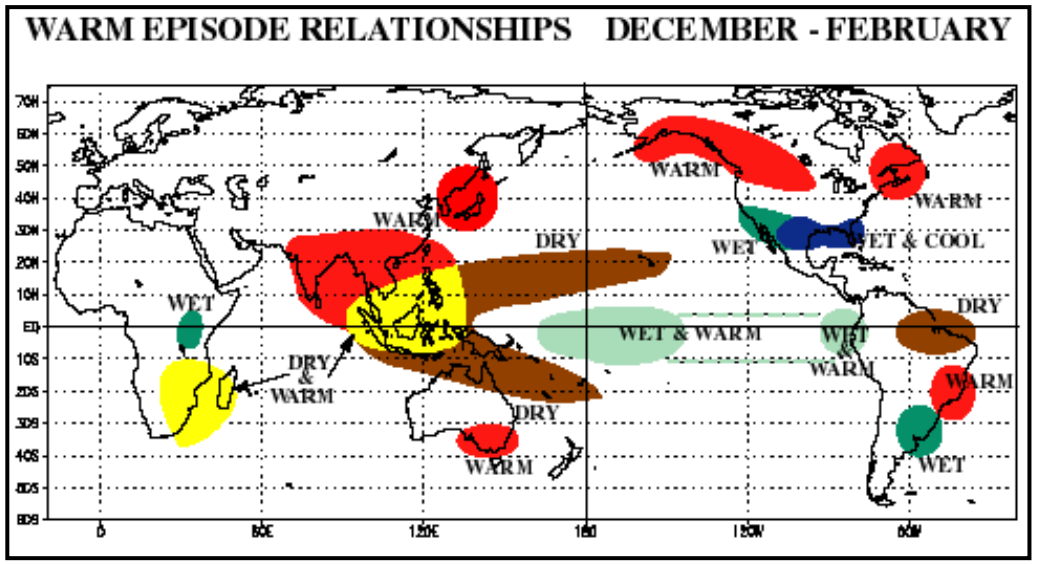

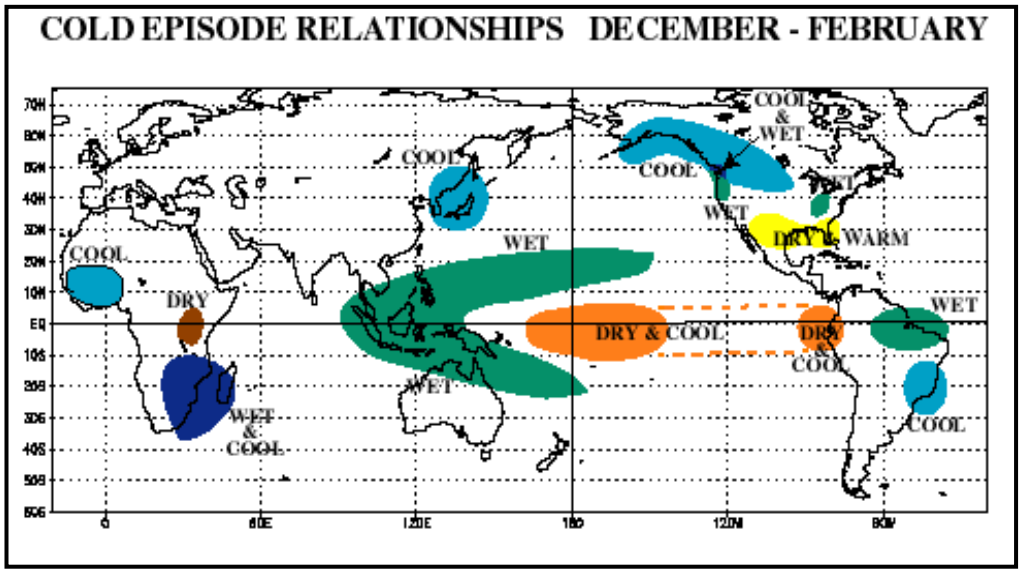

Extracted from CPC achieves

Carvalho et al 2002

EOFs of V200 (JFM)

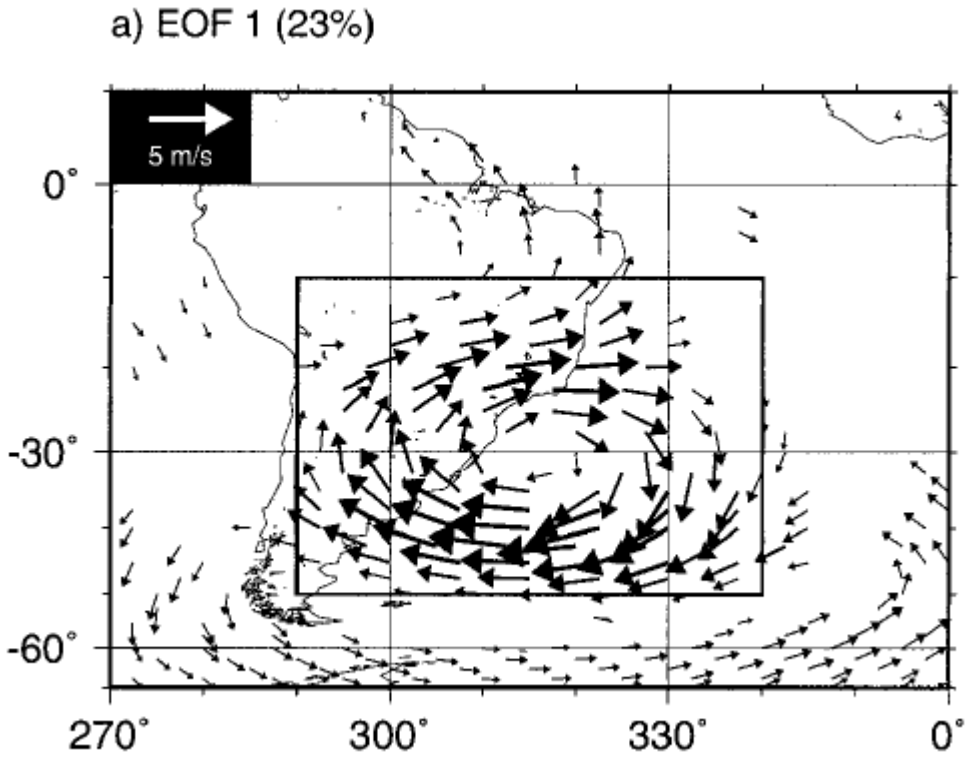

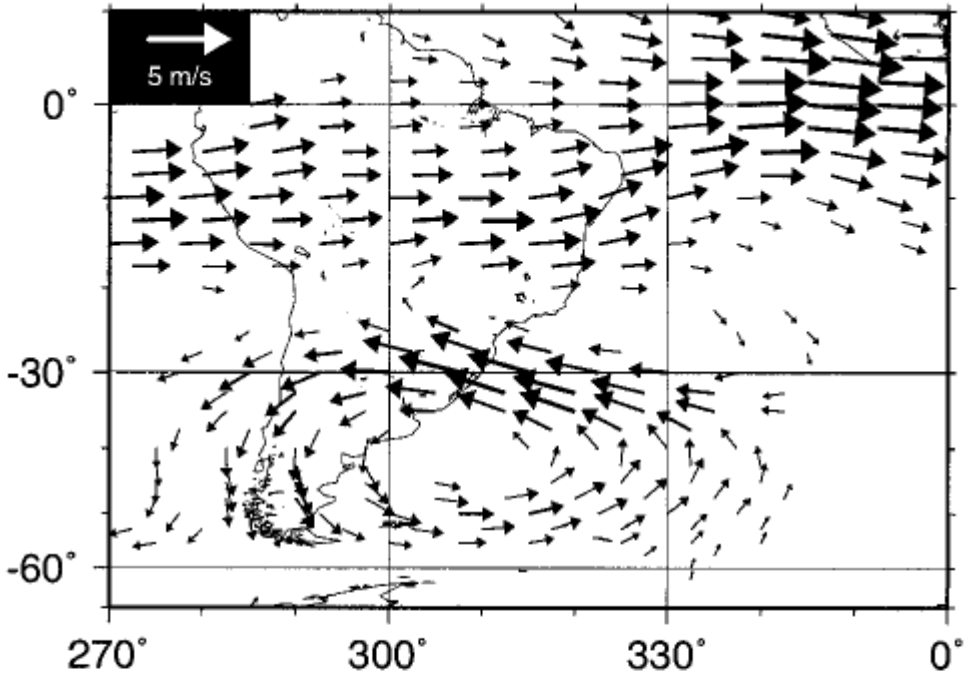

FIG. 2. Regression maps of 200-hPa winds with unfiltered (a) PC 1 and (b) PC 2. Magnitudes correspond to one standard deviation of the PC. The domain of the EOF analysis is indicated by the box in (a). Only vectors whose correlations with the respective PC pass a two-tailed Student t-test at the 95% level are plotted, with the number of effective degrees of freedom estimated locally at each grid point from the decorrelation times of the PC and the wind time series at that grid point (Davis 1976).

Robertson & Mechoso 2000

a) 500 hPa Omega & 200 hPa Wind

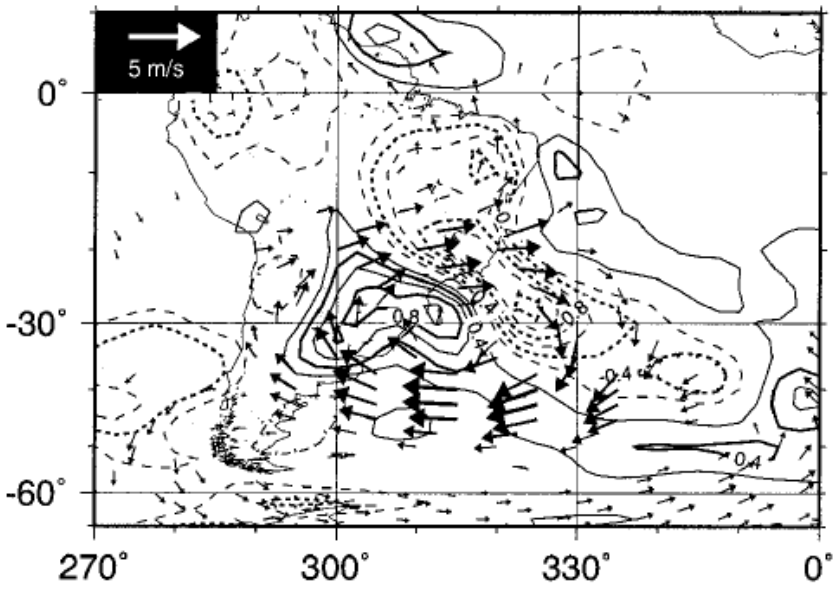

b) 850 hPa Temperature & Wind

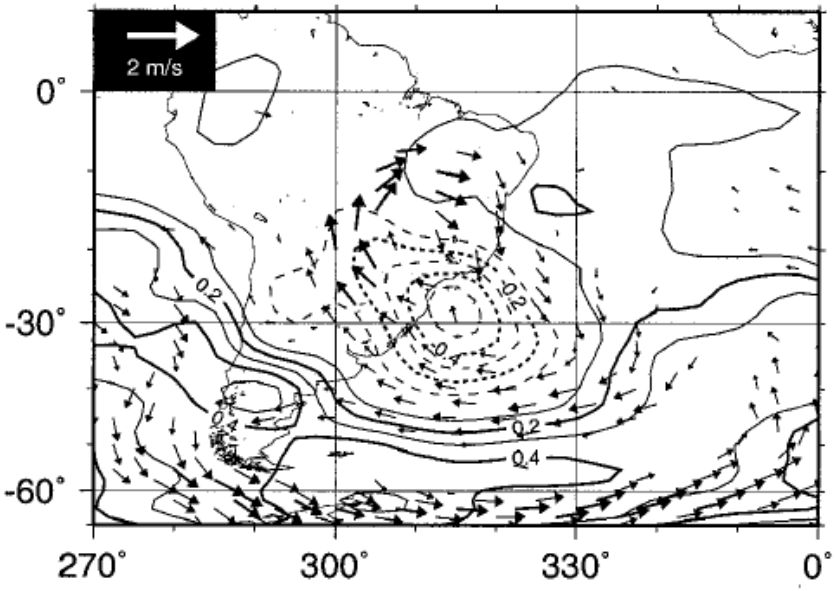

FIG. 3. Regression maps of PC 1 with (a) 200-hPa winds and 500-hPa omega (contour interval: 0.2 × 10^{-2} Pa s^{-1}), and (b) 850-hPa winds and temperature (contour interval: 0.1 K). Magnitudes correspond to one standard deviation of PC 1. Zero contour omitted and negative dashed.

- Dipolo en w500 con descenso al suroeste

- circulacion ciclonica en altura acompañada de circulacion ciclonica en superficie → barotropica.

- Nucleo frio del eddy.

- No hay correlacion con SPCZ ni con anomalias de V200 en otro lugar. → es un eddy aislado con caracteristicas de onda de Rossby estacionaria.

- Esta en balance de Sverdrup como vimos que vale en los tropicos? (Rodwell&Hoskins 2001; Gandu& Silva Dias 1998)
O sea: adveccion de vorticidad planetaria por flujo anomalo = estiramiento de vortices.

No esta en Sverdrup balance.

$$\overline{\mathbf{v}} \cdot \nabla \zeta' + \mathbf{v}' \cdot \nabla \overline{\zeta} = (\nabla \cdot \mathbf{v}')\overline{\zeta} + R_\zeta,$$

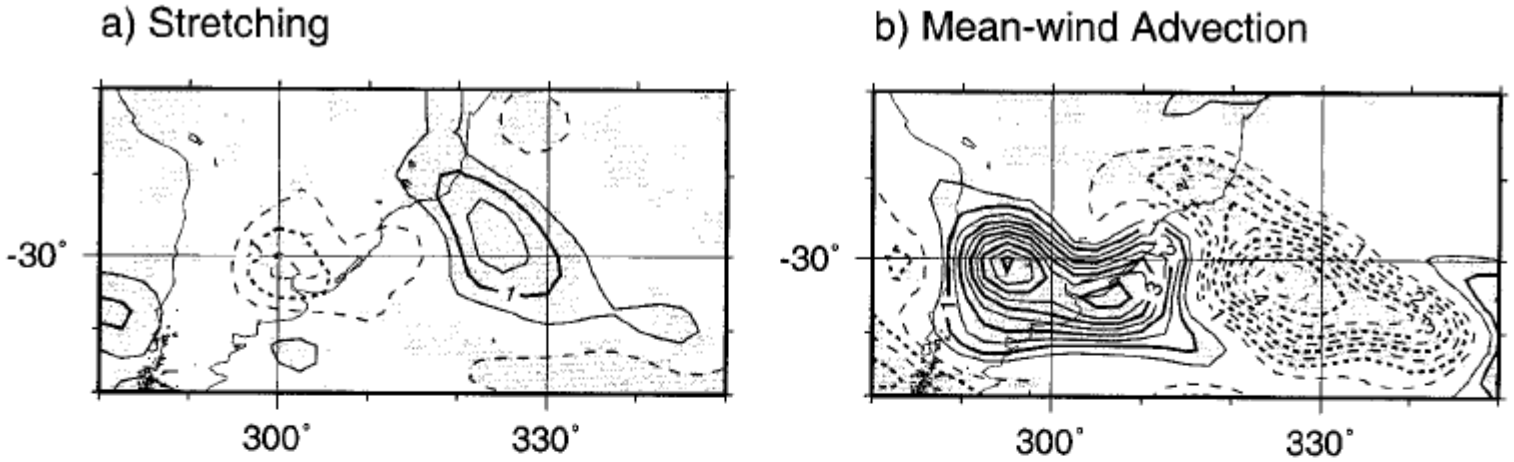

Adveccion de vorticidad relativa por el flujo medio (jet subtropical) balancea la adveccion de vorticidad planetaria por el flujo anomalo y el estiramiento de los vortices.

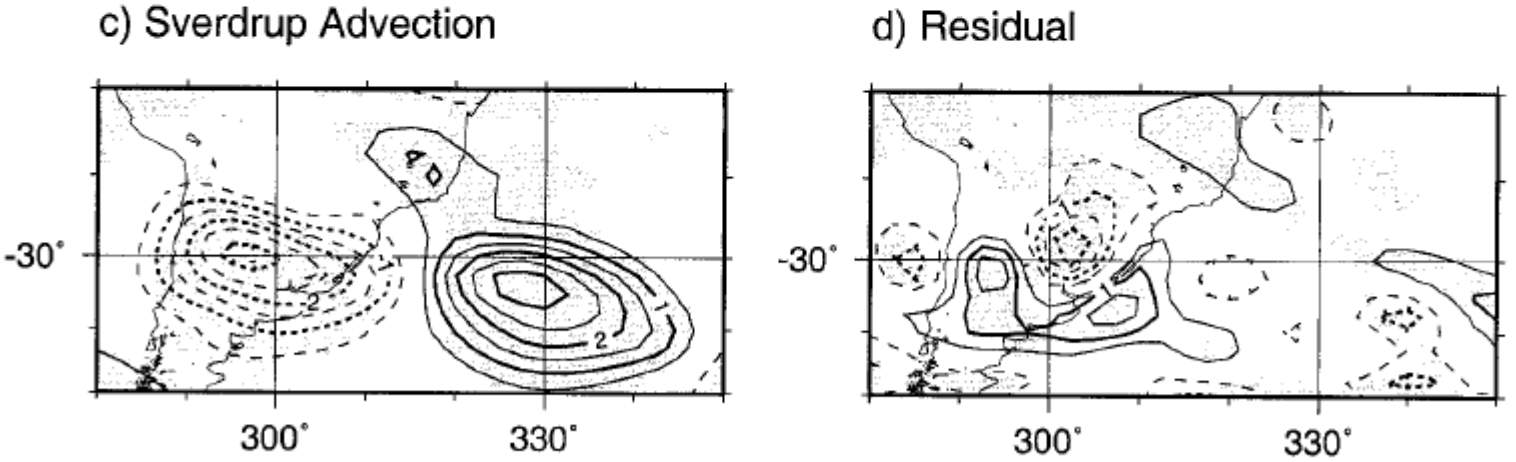

FIG. 4. Terms in the linearized vorticity budget at 200 hPa for the anomalously intense SACZ composite (see text). (a) $(\nabla \cdot \mathbf{v}')\overline{\zeta}$, (b) $-\overline{\mathbf{v}} \cdot \nabla \zeta'$, (c) $-\mathbf{v}' \cdot \nabla \overline{\zeta}$, and (d) R_ζ. The contour interval is 0.5×10^{-10} s^{-2}; zero contour omitted and negative dashed. Shaded areas are significant at the 95% confidence level, from a Student's two-tailed t-test with nine degrees of freedom.

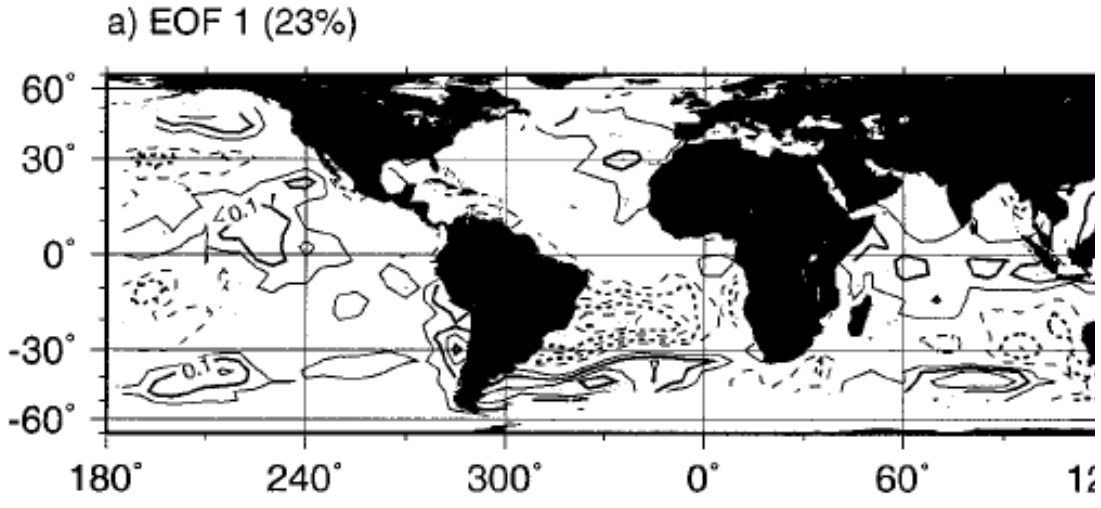

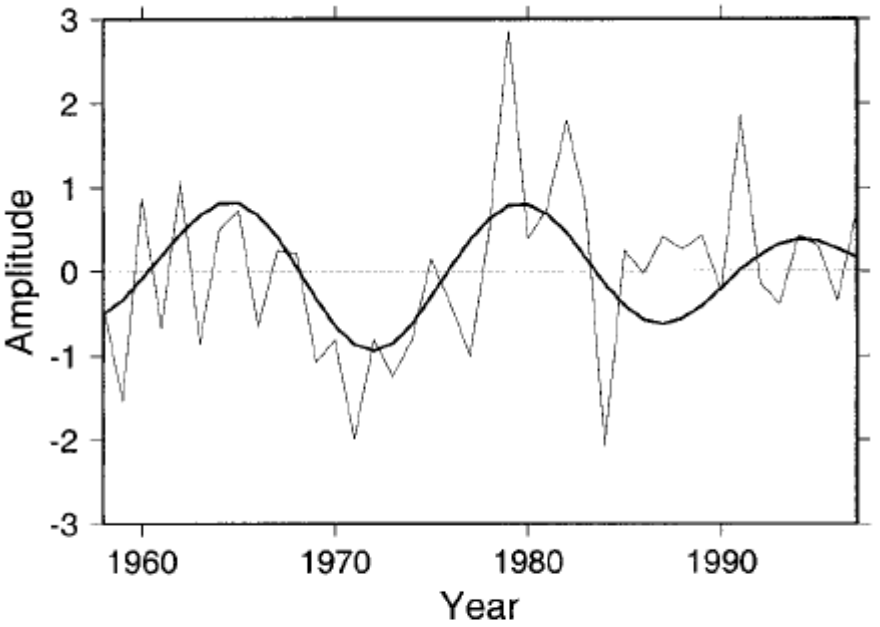

FIG. 8. Time series of PC 1 (light curve) and RCs 1–2 (heavy curve). The latter was constructed using an SSA with a window of $M = 20$ yr; the filtered series has a period of 14.7 yr and accounts for 24.5% of the variance. The units of the ordinate are standard deviations of PC 1. Years on the abscissa denote the JFM season.

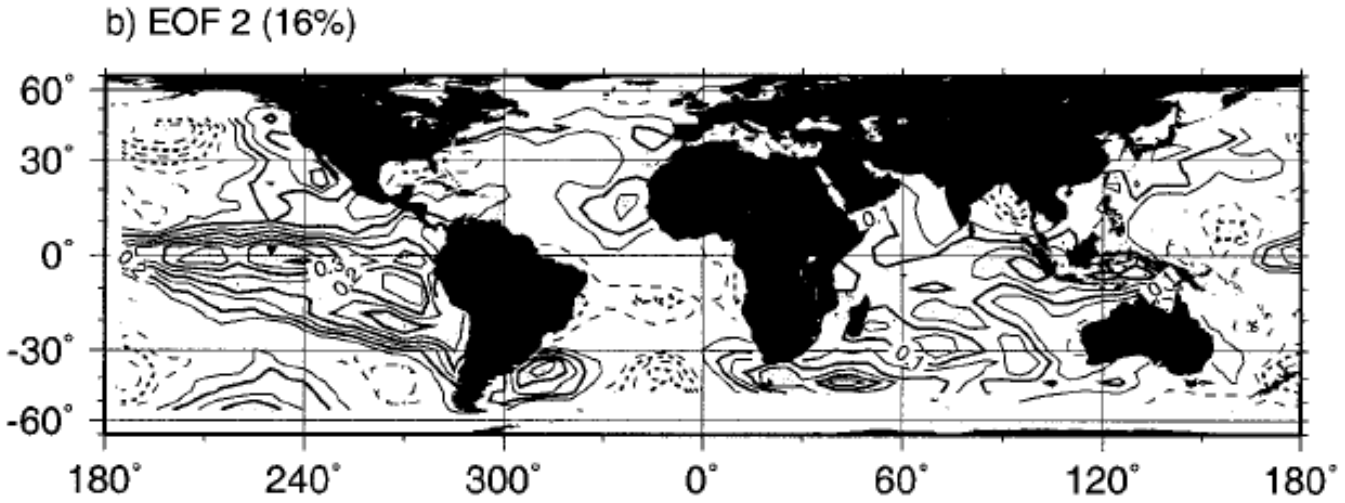

FIG. 7. Regression maps of SST with (a) PC 1 and (b) PC 2. The contour interval is 0.05 K, with the zero contour omitted and negative ones dashed. The shading denotes grid points whose associated correlations are significant at the 95% level, from a two-tailed Student's t-test with the number of degrees of freedom estimated on a pointwise basis as in Fig. 2.

Interacción ZCAS con TSM

- Robertson&Mechoso (2000) – Una ZCAS intensa enfría la TSM por debajo.

- Barreiro et al (2002, 2005) – La TSM puede influenciar la ZCAS en escalas interanuales y decadales moviendola hacia aguas cálidas.

- Chaves & Nobre (2004) - “feedback negativo”: una ZCAS intensa enfria la TSM a traves de una disminucion en radiacion y aumento de evaporacion. Luego esta TSM fria tiende a disminuir la actividad de la ZCAS (al menos la parte oceanica).

- Tirabassi et al (2014) – la TSM puede aumentar la persistencia de la ZCAS oceánica por unos días.

- Barreiro et al (2019) – la TSM interactúa con la ZCAS (refuerza anomalias y la corre al sur) en el contexto del impacto de la OMJ en Sudamérica.